

Reply to Reviewer Comment #1 from 19 August 2020

Thank you for the comprehensive second review of our study! We changed all small wordings and issues directly within the manuscript. All slightly bigger issues or separate comments are addressed below.

Detailed comments

L17:

We agree that it somehow doubles and is not necessary to distinguish this here in the abstract. We deleted the sentence and inserted a short explanation of the typical elevation change pattern.

L67: In the reply to reviewers comment you said that you added reference to Pamir to this sentence, but instead the words 'in particular' were added. I therefore assume that you meant to write 'in the Pamir' here?

You are right. This might have slipped through the back-checking and has been changed.

L84: Wording doesn't really make sense as written. Do you mean 'still connected'?

Yes, it should mean still connected and has been changed.

L96: The reply to reviewers document said that you had added a new section 3.4 to properly describe these maps, but it seems that didn't happen

Yes, this subchapter for the maps was indeed planned but later withdrawn as it was impossible to obtain the required more detailed information and because these maps are of limited relevance for the paper. However, we added a table with all map IDs in the supplement but forgot to mention it in the main paper and change it in the reply document. The information where to find the details has now been added.

L176: Explain what the numbers in brackets refer to in the paper.

We added an explanation earlier in the paper (former L123) where these numbers first occur.

L227: I think that you mean 'between' here (i.e., a glacier surge is a form of unstable flow, not separate from it?).

Yes, correct. We changed it to 'between'.

L316: It would make the values easier to identify if you added an equals sign ('=') before each one, as I've indicated above. At the moment I find the values for some of the categories a bit difficult to distinguish from the category descriptions that include numbers (e.g., for phase duration and terminus advance)

Yes that's right. It is more obvious to have some kind of a sign in between. We added a '=' as suggested.

L342: I found a 'leaves a large gap for' difficult to interpret, as it's a bit ambiguous as to whether it's referring to a lack of data or lack of surging glaciers. I think that you mean the latter, so this wording is better replaced with 'shows a lack of'.

Fully agreed and changed.

L399: I think you mean Fig. 11?

No, this is correct, we want to refer to Figure 10 where the surging glaciers are indicated on the map with black circles around the coloured disks.

L430: Expected compared to what? Provide ref(s)

We have changed it to than 'we' expected. We do not have a reference for it as this is likely the first time that such a number has been calculated. We had maybe expected 20 to 30 but not 50 to 130.

L457: I assume that this relates to a glacier ID, so it would be useful to include the glacier name or write something like 'glacier ID 41' to avoid any ambiguity

We have added 'ObjectID' to the number as above.

L474: Copland et al. (2011) also reported a large increase in glacier surging in the Karakoram over the period 1990-2014, compared to the 14 years before 1990, although I'm not sure if it's worth mentioning that here.

Yes, we think this study can be added here.

L535: Remind the reader what category 3, 2, and 1 refer to here (confirmed, probable, possible) to avoid any potential ambiguity given that the numbers mean different things in Sevestre and Benn (2015) vs RGI

We added the descriptions for the category 1 and 2 as category 3 is described in the text.

L737: Indicate what Criteria 1, 2 and 3 refer to in the caption.

As this scheme is rather complex for a caption, we have now added a note that refers the reader to the text for an explanation of these classes

L793: (a) label is partially obscured in the figure

Yes, thanks for the hint. The '(a)' is now visible again.

Reply to Reviewer Comment #2 from 25 August 2020

The authors revised the manuscript thoroughly considering almost all comments and thereby improved the coherence of the paper. Whether the inconsistencies in the data set itself have been corrected cannot be judged because the new version has not been provided. Therefore, I include my comments regarding the original version of the data set and strongly recommend checking the data base.

Data file GI-3min: I suggest to order the columns `dist_class`, `dur_class`, `srg_type` and `tongue` in the same order as in the `srg_code`. `Srg_type=2` (internal) and `dist_class>0` should not be possible, but there are many occurrences. I still have problems understanding `srg_duration`: There is one glacier (OBJECTID=10) with `srg_dur=300`. Is this a typo? Comparing glaciers 2 and 3, both starting in 1988, one has `dur_class=0` while the other one has `dur_class=3`. And for Bivachny, why is `srg_dur_y=7` and `dur_class=2` when both mapped surges were 2 years long?

Thank you for the comprehensive second review of our study! We reworked the dataset and it is now online.

Detailed comments

I. 27 "has recently received"

We changed it.

I. 78 Is "e.g." correct here?

Yes, it is correct (we considered also other studies).

I. 116 Better put height directly behind station name.

Yes, changed.

I. 122 "so far considered as not surging": Why so far? Do you mean surging or surge type here?

Yes, this is the question. It could be both but we are fine surge-type. 'so far' because nearly all of the largest glaciers are of surge-type there is at least one photograph where the surface of Fedchenko looks extremely 'surgy' but there is no further evidence. But if there will be further images available at some time (e.g. KFA1000) we might get further insights into the dynamics of Fedchenko.

I. 136 Now the Landsat list is the second table, but has no table caption. Should it be called S2 now?

Yes, we changed it in the text and also in the supplement.

I. 318 Add meaning of `duration=0`. Maybe I missed it, but how do you assign duration and distance for multiple surges with differing properties?

We explained this case directly before we presented the classification. It always refers to the main glacier body if there is more than one surge. Otherwise it would be too complex to display the properties and to create comprehensive attribute tables.

I. 363 Replace "almost the same area than" with "about the same area as", because almost implies smaller than.

Replaced.

I. 377 Change "mean elevation" to "median elevation" both times.

You are right, changed.

I. 416 There is an inconsistency: In the text you state: "For both graphs it has to be considered that the first period is including all glaciers". But in the caption of Fig 13 you say: "The "88-89" label in a) includes only glaciers that started surging in 1989".

Thank you for this hint. We changed the text, the caption is correct.

I. 422 Check which bars are black and which grey.

Thank you, we changed it to 'grey'.

I. 435 In fact, the 18% ONLY connect to another glacier in the maximum extent. The rest should be a tributary.

Yes, correct, we changed the text accordingly.

I. 436 Compare the numbers to the ones in the table (176 vs. 169).

Thank you for spotting, we have now changed the number in the text.

I. 439 Check numbers.

They are indeed in disagreement and have been corrected, thank you for the hint.

I. 444 Close parenthesis.

Closed.

Table 4: Check again the statement which surges are not listed. The ones with distance 0 should be the internal surging ones. But in the GI-3min there are also glaciers with dur_class=0, so the total number for duration classes 1-3 should not be 198.

Yes, you are right. This is still one issue of the automated calculation of the classes and has now been now fixed in the updated dataset.

Fig 11 Make sure that "(a)" is visible.

We made '(a)' visible again.

1 **More dynamic than expected: An updated survey of surging glaciers** 2 **in the Pamir**

3 Franz Goerlich¹, Tobias Bolch², Frank Paul¹

4 ¹Department of Geography, University of Zurich, Zurich, Switzerland

5 ²School of Geography and Sustainable Development, University of St. Andrews, St. Andrews, United Kingdom

6 *Correspondence to:* Franz Goerlich (franz.goerlich@geo.uzh.ch)

7 **Abstract.** The investigation of surging glaciers using remote sensing has recently seen a strong increase as freely
8 available satellite data and digital elevation models (DEMs) can provide detailed information about surges that
9 often take place in remote and inaccessible regions. Apart from analysing individual surges, satellite information
10 is increasingly used to collect valuable data on surging glaciers. Related inventories have recently been published
11 for several regions in High Mountain Asia including the Karakoram, parts of the Pamir and western Kunlun
12 Shan, but information for the entire Pamir is solely available from a historic database listing about 80 glaciers
13 with confirmed surges. Here we present an updated inventory of confirmed glacier surges for the Pamir that
14 considers results from earlier studies and is largely based on a systematic analysis of Landsat image time series
15 (1988 to 2018), very high-resolution imagery (Corona, Hexagon, Bing Maps, Google Earth) and DEM
16 differences. Actively surging glaciers were identified from animations and flicker images (e.g. terminus
17 advances) and the typical elevation change patterns. ~~Selected historic (Corona (lowering in an upper reservoir~~
18 ~~zone and Hexagon) and contemporary very high-resolution imagery (Bing Maps and Google Earth) were used to~~
19 ~~confirm surges thickening further down in a receiving zone).~~ In total, we identified 206 spatially distinct surges
20 within 186 glacier bodies, mostly clustered in the northern and central part of the Pamir. Where possible,
21 minimum and maximum glacier extents were digitized, but often interacting tributaries made a clear separation
22 challenging. Most surging glaciers (n=70) are found in the larger size classes (>10 km²), but two of them are very
23 small (<0.5 km²). We found also several surges where the length of the glacier increased by more than 100%.
24 The created datasets are available at: <https://doi.pangaea.de/10.1594/PANGAEA.914150> (Goerlich et al., 2020).
25

26 **1 Introduction**

27 The investigation of surging glaciers using satellite data has ~~recently~~ received ~~recently~~ increased attention among
28 scientists, in particular for the Karakoram mountain range but also other regions of the world (e.g. Berthier and
29 Brun, 2019; Bhambri et al., 2017; Bolch et al., 2017; Falaschi et al., 2018; Minora et al., 2016; Paul, 2015 and
30 2020; Quincey et al., 2015; Rankl and Braun, 2016; Round et al., 2017; Steiner et al., 2018). This has several
31 reasons, for example (a) the free access to long (Landsat) and dense (TerraSAR-X / TanDEM-X, Sentinel-1/2)
32 time series of high-resolution satellite data, (b) the limited understanding of why some glaciers in this region are
33 surging while others do not, (c) a large number of on-going surges at any point in time, (d) the large variations of
34 surge behaviour in a small region, (e) the long history of still occurring surge-related hazards (mostly due to
35 damming of a river and related outburst of lakes), and (f) the very difficult field access. Thereby, most studies

36 document the variations in glacier extent / length changes, flow velocities and elevation / mass changes in the
37 course of a surge or surge-related hazards. These studies have revealed unprecedented details about surge
38 dynamics and variations that have already helped in improving our understanding of related surge mechanisms.

39

40 In contrast, the surging glaciers in the Pamir mountain ranges to the north of the Karakoram received less
41 attention, but recently some studies were published (e.g. Lv et al. 2019; Osipova 2015; Wendt et al. 2017; Holzer
42 et al. 2016). This might be due to the fact that several surges during the Soviet era have already been described in
43 detail (e.g. the surges of Medvezhy and Geographical Society glaciers are well documented, see Dolgushin and
44 Osipova (1971, 1975), Kotlyakov et al. (2003) and Osipova (2015)) and a detailed inventory describing a high
45 number (>800) of surge-type glaciers based on satellite data and aerial images was published (Osipova et al.
46 1998). However, this and many of the publications are in Russian and are therefore little known internationally.

47

48 When speaking about surging glaciers, we first have to differentiate between surge-type glaciers and other
49 glaciers. This is important when interpreting glacier changes in the context of climate change, e.g. their length or
50 mass changes over a time period when surges have occurred (Bolch et al., 2017; Brun et al., 2017; Gardelle et al.,
51 2013). Secondly, it is also important to distinguish surge-type from surging glaciers. The former have surged at
52 some point in the past and show indirect ~~evidencesevidence~~ like looped or distorted moraines or post-surge
53 down-wasting features of a former surge, whereas the latter surged actively within the observation period.
54 Looped or otherwise distorted moraines occur due to former surges that pushed the lobate-shaped boundaries of
55 tributaries ~~downward-indicated~~ down glacier, indicating different flow speeds among major, moraine-separated
56 glacier branches (Herreid and Truffer, 2016; Meier and Post, 1969). The typical post-surge down-wasting
57 features ~~are~~ consist of separated lower glacier parts and/or the jagged boundary of a stagnant and rapidly lowering
58 glacier tongue, among others (Paul, 2020). We here only investigate glaciers that have actively surged during the
59 observation period. The globally most complete compilation of surge-type glaciers by Sevestre and Benn (2015)
60 is a ~~most~~-valuable starting point, but it is based on literature sources up to the year 2013 only. In the meantime,
61 numerous ~~further~~ other surge-type glaciers have been identified across High Mountain Asia (HMA) from the
62 analysis of multi-temporal satellite imagery, e.g. in the Karakoram (Bhambri et al., 2017), Kunlun Shan (Yasuda
63 and Furuya, 2015), central Tibet (Zhang et al., 2018), eastern Pamir (Lv et al., 2019) and Tian Shan (Mukherjee
64 et al., 2017), but an update of confirmed surges for the entire Pamir Mountains is yet missing. With this study we
65 aim ~~at identifying~~ to identify them and provide detailed information (e.g. timing and typology) about confirmed
66 glacier surges in the Pamir Mountains.

67

68 Surge-type glaciers in ~~particular~~ the Pamir are included in the inventory by Osipova et al. (1998) and Sevestre and
69 Benn (2015). There are thus important differences in our approach compared to the methodology used for the
70 ‘catalogue’ by Osipova et al. (1998), implying that both are not directly comparable: (i) our satellite image time
71 series (Landsat) has a lower spatial resolution (30 m) than the KFA1000 data (3-5 m) used by Osipova et al.
72 (1998), (cf. also Dowdeswell et al. 1993, 1995), (ii) we cover a different period (1988–2018) than Osipova
73 (1998), ~~have~~-(iii) we have used different indicators for surge identification (e.g. animations, DEM difference
74 patterns), (iv) we have assigned only one surge class instead of six- and (v) our glacier entities have different

75 boundaries as we used the most recent Pamir glacier inventory by Mölg et al. (2018) as a base for the analysis
76 (here named GI-1).

77

78 The information from Osipova et al. (1998) is also available in the Randolph Glacier Inventory (RGI) version 6
79 (RGI Consortium 2017) using the simplified classification scheme developed by Sevestre and Benn (2015). We
80 have used the RGI dataset and revisited existing literature, e.g. ~~and~~ the study by Lv et al. (2019), as a starting
81 point for our inventory of glacier surges. Our analysis is primarily based on animated multi-temporal (1988-
82 2018) time-series of Landsat data, but also on elevation difference maps showing the typical mass transfer pattern
83 of glacier surges. For some less clear cases, we also analysed very high-resolution images from the Corona and
84 Hexagon missions and the images in Google Earth and Bing Maps for confirmation.

85

86 For this study, we revisited the GI-1 inventory by adding ice divides for glacier units that surged but were so far
87 still connected with other glaciers in GI-1, resulting in a new inventory GI-2. In a second step, three inventory
88 subsets are created from GI-2 that provide (a) the selection of surging glaciers only (GI-3), (b) minimum (GI-
89 3min), and (c) maximum (GI-3max) extents of all surging glaciers. In the following, the number in brackets after
90 a glacier's name refers to its ID in the GI-3min inventory. We also present a rough classification of the different
91 surge-types, the timing of surges during the observation period (1988-2018), a comparison of geomorphometric
92 characteristics (other glaciers in GI-2 vs. GI-3), and a description of geometric changes due to a surge.

93 **2 Study region**

94 The Pamir is one of highest mountain ranges within HMA and of the world extending from about 36°35' to
95 39°35' N and 70°35' to 75°35' E (Fig. 1). The northern part belongs to the Osh region of Kyrgyzstan, the eastern
96 parts to the Xinjiang Uighur Autonomous Region of China, the most southern regions to Badakhshan in
97 northeastern Afghanistan and the main part to Gorno-Badakhshan in Tajikistan. The highest peak (Mt. Kongur)
98 reaches up to 7649 m a.s.l. and enthrones over the Kongur Shan in the eastern part of the Pamir ~~(at~~ Here and in
99 the following we use names ~~are based on selected from~~ transliterated Russian topographic maps at a 1:500.000
100 ~~and 1:100.000~~ scale (see Table S1 in the Supplement).

101

102 *Figure 1*

103

104 Typical glaciers in the Pamir are long and dendritic or multi-basin valley glaciers, but other types such as
105 mountain glaciers and cirques exist as well. Due to the steep and ice-free surrounding rock walls, most glaciers
106 are at least partly debris covered, which often simplifies the identification of typical surge marks (e.g. looped
107 moraines) from space (e.g. Kotlyakov et al. 2008). Most glaciers are concentrated in the central part around
108 Ismoil Somoni Peak (7495 m a.s.l.) including Fedchenko Glacier, which is with a length of >70 km the longest
109 valley glacier in the world outside the polar regions (Machguth and Huss, 2014). Additionally, the region is home
110 ~~to~~ abundant rock glaciers that are not always clearly separable from debris-covered glaciers and other ice-
111 debris landforms (Mölg et al., 2018).

112

113 The glaciers in the western and central part of the Pamir (Tadjik, Kyrgyz and Afghan regions) are of winter
114 accumulation type where most precipitation (~90%) falls between December and May (Maussion et al., 2014)
115 with annual amounts of up to 1285 mm a⁻¹ at Fedchenko weather station at 4169 m.a.s.l. (Finaev et al., 2016).
116 Conversely, the glaciers in the eastern part are mainly (50 to 60%) fed by precipitation in the summer months
117 between June and August, which can be seen as an effect of the monsoon (Maussion et al., 2014). The total
118 annual precipitation is very low in some regions, reaching only ~70 mm a⁻¹ at Murgab (3576 m a.s.l.) and
119 Toxkargan ([3090 m a.s.l.](#)) weather stations, both located in valleys (~~3090 m a.s.l.~~) (Finaev et al., 2016). Hence,
120 the glaciers in the western and central part are situated in a somewhat warmer and more humid climate whereas
121 the eastern ranges are dry and cold. Accordingly, glacier mean elevations of the former can be found at lower
122 altitudes (~4740 m a.s.l.) than in the eastern regions (~5050 m a.s.l.) according to the dataset presented by M \ddot{o} lg
123 et al. (2018).

124

125 The likely best-investigated glacier in the region is Fedchenko (Lambrecht et al., 2014, 2018) that is so far
126 considered as not ~~surging-of surge-type~~. Of the glaciers with confirmed surges, Medvezhy Glacier (29, [ObjectID](#)
127 [in the GI3-min inventory](#)) is likely the best investigated (see Kotlyakov et al., 2008). This latter study also
128 reported details about surges of several other glaciers in the region, partly back to 1959.

129 **3 Datasets and pre-processing**

130 **3.1 Satellite data**

131 **3.1.1 Landsat**

132 For the detection of glacier surges and determination of surge start, end and possibly their full surge cycle (e.g.
133 from the starting year of an active phase to the start of the next active phase), we used freely available Landsat
134 imagery (Level 1T) from earthexplorer.usgs.gov including Landsat 5 TM (Thematic Mapper), Landsat 7 ETM+
135 (Enhanced Thematic Mapper plus) and Landsat 8 OLI (Operational Land Imager) sensors. Additionally, we used
136 some very good scenes (no snow outside glaciers) from Landsat MSS (Multispectral Scanner) from the 1970s
137 and 1980s. The three sensors TM, ETM+ and OLI acquire data with a horizontal resolution of 30 m for the
138 visible, near-infrared (NIR) and shortwave infrared (SWIR) bands at a repeat rate of 16 days. Key characteristics
139 of the datasets are shown in Table 1; the full list of scenes used for this study is presented in Table ~~S1~~[S2](#) in the
140 Supplementary Material.

141

142 In general, cloud-free scenes from the end of the summer (July to October) are used from all sensors, but for
143 some regions, also earlier acquisitions are considered to have images available for as many years as possible.
144 With a focus on the changes near the glacier terminus, the remaining seasonal snow at higher elevations in these
145 images was unproblematic. Unfortunately, it was not possible to find suitable scenes for each year in most
146 regions so that the determination of the onset or end of a surge has at least a ± 1 year uncertainty. Priority was
147 given to Landsat 5 TM scenes to limit using Landsat 7 ETM+ scenes after 2002 when the Scan Line Corrector
148 (SLC) stopped working (resulting in so-called SLC-off scenes). For the animations we downloaded the standard

149 colour-balanced and orthorectified image quicklooks from earthexplorer.usgs.gov that are provided in false-
150 colours (glacier ice and snow is depicted in cyan) and at the original resolution. The jpg-compression of these
151 images results locally in blurred details but they had only a very small impact on surge identification.

152

153 *Table 1*

154

155 **3.1.2 Corona and Hexagon**

156 The Corona Keyhole (KH) 4B scenes from August 1968 (Table S1) cover the central and northern Pamir (see
157 Fig. 1) and were also downloaded from earthexplorer.usgs.gov. The Corona images are panchromatic, recorded
158 in stereo mode and have a ground resolution of up to 1.8 m (Galiatsatos, 2009). We processed 11 scene pairs to
159 generate a DEM and corresponding orthophotos with 5 m resolution following Goerlich et al. (2017). Due to the
160 high effort of processing the scenes, the orthoimages only cover the region with the most surging glaciers. The
161 orthoimages revealed details in surface morphology that are typical for surging glaciers but barely visible for the
162 largest glaciers at the 30 or 15 m resolution of Landsat images. We also used Hexagon KH-9 scenes from July
163 1975 and June 1980 to generate orthoimages following Pieczonka et al. (2013). The scenes depict the regions
164 west of lake Karakul with a resolution of up to 6 m.

165 **3.1.3 Google Earth and Bing Maps**

166 The very high-resolution (a few m or better) satellite images available in Google Earth (GE) have been widely
167 used for numerous geoscientific applications (Liang et al., 2018). We used them here together with the satellite
168 images available on Bing Maps to confirm identified surging glaciers in the Landsat period, i.e. for visual checks
169 only. Sometimes the available time series in GE also allowed a proper identification of glacier surges when the
170 quiescent and/or active phases are captured (see examples in Lv et al., 2019). Interestingly, the images used in
171 Bing Maps were often complimentary to GE, i.e. provided excellent coverage when nothing useful was available
172 in GE and vice versa.

173

174 In Fig. 2 we provide a visual comparison of image sources displaying three surging glaciers in the central Pamir
175 to illustrate the visibility of details. We include examples from Corona, Hexagon, Landsat OLI as well as GeoEye
176 (from Bing Maps). The high-resolution images from Corona and Bing Maps clearly show the highly crevassed
177 surfaces (mainly for the two larger glaciers) that are not visible in the Landsat image. In the Landsat image, the
178 glacier boundary and debris-covered parts can be identified, but it is almost impossible to reveal the terminus of
179 Walter 731 (19) and Soldatov (20) glaciers in the static image. This is different when using animations that reveal
180 glacier termini clearly when they change position (Paul, 2015).

181

182 *Figure 2*

183

184 3.2 Digital elevation models (DEMs)

185 Several DEMs are freely available for the study region. This includes the Shuttle Radar Topography Mission
186 (SRTM) DEM (Rabus et al., 2003), the Advanced Spaceborne Thermal Emission and Reflection Radiometer
187 (ASTER) GDEMv3 (NASA, 2018), the ALOS PRISM DEM AW3D30 (Takaku et al., 2014), the High Mountain
188 Asia (HMA) DEM (Shean, 2017) and the DEM from the TanDEM-X mission (TDX) provided by DLR (German
189 Aerospace Centre) (Wessel, 2016). They have different characteristics (sensor types, spatial resolution, artefacts,
190 data voids, acquisition dates) and – apart from the HMA DEM – are used here for several purposes such as
191 calculation of topographic characteristics and surface elevation changes (Table 2). A direct comparison of the
192 DEMs using hillshades and DEM differences revealed that only the GDEMv3 and the AW3D30 DEM are free of
193 data voids but that the AW3D30 has partlysome artefacts over glacier surfaces and too high elevations. We thus
194 used the GDEMv3 to determine topographic characteristics for all glaciers.

195

196 Besides the orthoimages, we created DEMs from the 1968 Corona stereo pairs (cf. Goerlich et al., 2017) and used
197 DEMs from 1975 Hexagon data (cf. Pieczonka et al., 2013). The AW3D30 DEM served as a height reference
198 (Ground Control Points, Disparity Predictions) for the Corona DEM processing and the SRTM DEM for
199 Hexagon. The main difference of the final DEMs is the coverage where Corona covers only a small area (~15 km
200 x 180 km) per stereo image pair compared to Hexagon (~130 km x 130 km). This results in a far larger effort to
201 generate DEMs and orthophotos from Corona for a larger region.

202

203 We have used the temporarilytemporally better constrained DEMs from Corona (1968), SRTM (2000), AW3D30
204 (2006-2011), and TDX (2011-2014) to determine elevation changes over the periods of 1968 to 2000, 2000 to
205 ~2009, and ~2009 to ~2012/14. Elevation differences were interpreted in a qualitative sense only as the typical
206 pattern of elevation changes for surging glaciers (strong elevation gain in the lower and loss in the upper region
207 during the active phase of a surge, and vice versa for the quiescent phase) can be clearly identified in most cases,
208 i.e. changes are often much higher (100+ m) than the combined uncertainties of the two DEMs (e.g. Gardelle et
209 al. 2013).

210

211 *Table 2*

212

213 3.3 Glacier outline datasets

214 We used the Karakoram / Pamir glacier inventory (GI-1) created by Mölg et al. (2018) as a basis for glacier
215 identification and extent modification. This inventory provides a consistent dataset of manually corrected glacier
216 outlines based on Landsat scenes acquired between 1998 and 2002 for the entire Pamir, including the ranges
217 Kingtau, Ulugarttag and Muztagh in the Chinese part (see Fig. 1). As the inventory is a temporal snap shot and
218 surge-type glaciers are in various stages of their surge cycle, they can be connected to a larger main glacier and
219 thus not be analysed separately. To overcome this restriction, we have separated all part-time tributaries
220 exhibiting their own dynamics from the glaciers they connect with and added the required new ice divides in the
221 accumulation regions. This revised inventory (GI-2) is used as the base for all subsequent geomorphometric

222 calculations. The separation follows the natural flow and extent of the larger glacier and required several
223 iterations of adjustments, as the surge characteristics were often not clear from the beginning. After all surges
224 have been identified, a sub-sample of GI-2 was created that only includes the glaciers that surged (inventory GI-
225 3). The GI-3 sub-sample served as a base to digitise minimum and maximum glacier extents for all glaciers
226 exhibiting a visible change in terminus position. These datasets are saved in two additional inventories (GI-3min
227 and GI-3max, respectively).

228 **4. Methods**

229 **4.1 Surge identification**

230 Glacier surges can occur in very different forms with a likely continuous transition ~~to~~between unstable flow and
231 regular glacier advances. Hence, a clear identification of surge-type glaciers is not trivial even in their active
232 phase and a wide range of identification criteria has been suggested to distinguish them from all other glaciers
233 (e.g. Sevestre et al., 2015; Bhambri et al., 2017; Mukherjee et al., 2017). In this study, we focus on glaciers that
234 had an active surge phase during the investigated period 1988-2018, i.e. indirect evidences alone such as distorted
235 or looped moraines are not considered. Consequently, our sample is smaller than the one presented in the
236 ‘catalogue’ by Osipova et al. (1998), who listed 845 surge-type glaciers for the Pamir (i.e. 35% of the global
237 sample by Sevestre and Benn (2015)) in six distinct classes. Their inventory is also digitally available in the RGI
238 using the simplified classification scheme by Sevestre and Benn (2015), with the classes (their Table 4):
239 confirmed (Category 3), probable (2) and possible (1). With our focus on observed surges (with few exceptions)
240 our sample would be in the ‘confirmed’ type of which Osipova et al. (1998) list 61 and Sevestre and Benn (2015)
241 90 glaciers.

242

243 To identify surging glaciers, we started with the ‘confirmed’ samples listed by Osipova et al. (1998, 2010),
244 Kotlyakov et al. (2008) and Lv et al. (2019). These studies included all mountain ranges where we searched for
245 surging glaciers except the Rushanskii and Muztagh ranges. Our identification consists of four steps:

246

247 (I) At first, we analysed animations from the Landsat quicklooks to validate the findings of the four studies. Each
248 frame set was animated with slightly different samples (varying selection of animated scenes within one frame
249 set) to facilitate visibility of glacier dynamics in each region similar to Paul (2015). The qualitative analysis
250 tracked surface feature displacements and was applied to the entire study region. Collectively, this step revealed
251 139 surging glaciers during the period 1988-2018 (including glaciers that have just started surging).

252 (II) In the next step, we analysed the elevation change patterns of the various DEM difference maps in a
253 qualitative way (Mukherjee et al., 2017). Glaciers showing the typical opposing pattern of surface elevation
254 change along the glacier ~~flow~~flowline (lowering and thickening) were digitally marked and added to the sample,
255 yielding 35 further glaciers from the 1968 to 2000 and 2000 to c. 2009 elevation difference maps. For this
256 analysis it does not matter in which region of a glacier the pattern occurs (e.g. internal surges may appear higher
257 up and do not reach the terminus). Two examples of the related DEM difference maps are displayed in Fig. 3,

258 revealing for some glaciers the typical surge pattern. This method helped in detecting internal surges with limited
259 or no changes of the terminus position and/or where crevasses or shear margins are difficult to detect.

260

261 *Figure 3*

262

263 (III) In this step, we analysed individual image pairs in detail using flicker images, i.e. going back and forth
264 between two images only (Kääb et al. 2003). For a clear before/after distinction, this analysis was restricted to the
265 best scenes available for a specific region (e.g. without clouds, seasonal snow or deep shadows). We here also
266 used the contrast-enhanced false colour infrared images from the MSS scenes, several 15 m panchromatic images
267 of ETM+ and OLI and the declassified orthoimages. An additional 27 surging glaciers could be identified this
268 way.

269

270 (IV) In the final step, we checked the identified glaciers with the partially very high-resolution images available
271 in GE and Bing Maps to also analyse morphological characteristics of the glacier surfaces in detail, their shape
272 and also possible changes in extent (Lv et al., 2019). Despite the variability in acquisition years, this allowed us
273 to remove a few glaciers (7) from the sample (in most cases the ‘surges’ were likely just advances) and also
274 ~~adding~~ 12 new ones. We ~~decided for~~classified a glacier ~~advances~~advance as when the glacier does not show
275 any of the typical surface features such as a heavily crevassed surface, shear margins or collapsing/down-wasting
276 patterns at the tongue and a comparably small and/or slow advance. At this stage, we started introducing indirect
277 evidence (surface features) to the classification and thus checked back if the (mostly small) glaciers have really
278 surged using animations. In some cases it was necessary to interpret results from steps (I) to (III) collectively for
279 a reasonable result.

280

281 Based on the created inventory subset with surging glaciers only (GI-3), we digitised the minimum (GI-3min)
282 and maximum (GI-3max) extent of all glaciers based on the satellite images described in Section 3.1. For glaciers
283 with more than one surge, the respectively largest and smallest extents were digitised (Fig. 4). Whereas
284 maximum extents are in most cases well identifiable, outlines for GI-3min can have larger uncertainties due to
285 the difficulties in clearly identifying the new terminus among the often debris-covered and down-wasting ice
286 from the previous surge. Ideally, the minimum extent is identified once the next surge has started, but for many
287 glaciers this did not happen during the observation period.

288

289 *Figure 4*

290

291 **4.2 Surge characteristics and classification**

292 There are a wide range of possibilities to characterise surges as they have a high variability of appearance and
293 dynamics (e.g. Bhambri et al. 2017). For the GI-3min inventory we have determined a series of key surge
294 characteristics in the attribute table (e.g. surge start / end / duration, and distance) and a simplified classification
295 according to a pre-defined criteria set for statistical analysis and comparison with other regions. It has to be noted

296 that a precise start/end year was often difficult to determine either due to missing satellite data, but also when
297 surge initiation is related to a mass wave coming down from higher elevations (taking a few years) or when
298 remaining dead ice from a previous surge was reactivated. We here defined the start of a surge as the year when
299 an advance of the terminus or a mass wave higher up the glacier (as not all surges show a terminus advance) is
300 detectable. The end of the active phase (maximum extent) is reached when all surge dynamics settle and the
301 quiescent phase begins. The surge duration is calculated by subtracting the start year from the end year of the
302 surge. The latter was easier to determine than minimum extents in most cases.

303

304 To illustrate a few of the possible surge types and interactions, Fig. 5 displays a sketch map of three glaciers that
305 are all surging at some stage. Starting with a surge of the permanently connected tributary (2) in Fig. 5a, this
306 surge is at its maximum extent in Fig. 5b and the ice from the surge is already slightly moved downstream by the
307 flow of the main glacier (1). In addition, glacier (3) started surging in the meantime, connects to the main glacier
308 in Fig. 5b and enters glacier (1) in Fig. 5c where it also reaches its maximum extent. Some time later (Fig. 5d),
309 also the main glacier (1) is in full surge mode and transports the surge marks of both tributary surges
310 downstream, stretching and possibly deforming them. This illustrates the variety of surge interactions (by far not
311 all) and the difficulty to define maximum extents of tributary glaciers. Their surge marks are moved downstream
312 by the main glacier during or near the end of their own surge due to its normal flow or a surge of the main
313 glacier. Accordingly, there is also some uncertainty in the timing of the surge end for glaciers (2) and (3). In this
314 case the main glacier body (1) would have listed two surges in the attribute table of GI-3min and would have
315 been selected to receive the surging classification code.

316

317 *Figure 5*

318

319 For the classification scheme, we used the following criteria and values for each glacier:

320 (A) ‘surging?’: no \equiv 0, yes \equiv 1, if yes:

321 (B) glacier tongue: free end \equiv 1, connects to another glacier \equiv 2, tributary \equiv 3

322 (C) type of surge: advancing \equiv 1, internal \equiv 2, combined \equiv 3

323 (D) active phase duration: 1-3 years \equiv 1, 4-10 years \equiv 2, >10 years \equiv 3

324 (E) terminus advance: none \equiv 0, short (<1 km) \equiv 1, medium (1-2.5 km) \equiv 2, long (> 2.5 km) \equiv 3.

325 In (C), the ‘advancing’ type defines a glacier that has a visible terminus change, ‘internal’ has no advance but
326 either a visible mass wave in the Landsat images or in the DEM difference images. The combined type describes
327 glaciers that show a mass wave within the glacier reaching the terminus and pushing it further down valley.

328 Hence, the entry in the attribute table of GI-2 is either 0 or 1 and stored in a separate ‘surge’ column. The
329 resulting code from our classification in GI-3min is then for example 2123. This means that the glacier is
330 connected to another glacier during its surge, that it has an advancing tongue and surged over a period of 4-10
331 years over a long distance. In the case the glacier already surged in 1988 or was still surging in 2018, these two
332 years were used as the start or end date. Such dates indicate that the real surge duration is likely longer than given
333 in the table.

334 4.3 Topographic and other information

335 For all glaciers in GI-2, we calculated the following attributes according to Paul et al. (2002, 2009): centre point
336 latitude and longitude, area in km², minimum, maximum, mean, and median elevation, mean slope and aspect,
337 and aspect sector. Mean values are calculated as the arithmetic average of all DEM cells covered by the
338 respective glacier. All attributes are also transferred to GI-3, and additionally calculated for GI-3min and GI-
339 3max. The attributes of GI-2/GI-3 depict the glacier state around the year 2000. For GI-3min/GI-3max the
340 attribute date varies between 1988 and 2018 due to the minimum and maximum extent of the glaciers. All
341 elevation dependent attributes are based on ASTER GDEMv3 elevations.

342 5. Results

343 5.1 Distribution and topographic characteristics of surge and other glaciers

344 From the ~13500 glaciers in the study region, 186 have been identified as surging glaciers of which 206 spatially
345 distinct surges have been identified between 1988 and 2018. Their occurrence is clustered in the central, northern
346 (central and western Pamir Alai, Fedchenko and ‘Petr Alervogo East’) and eastern ranges (Muztagh and
347 Ulugarttag) (Fig. 6). This pattern leaves shows a large gap ~~for of~~ glacier surges around Lake Karakul and to the
348 south of the study region with few exceptions. Overall, ~~the these~~ latter regions are dominated by comparably
349 smaller glaciers and drier climate, indicating that there might be a size and climatic threshold for surge activity as
350 suggested by Sevestre and Benn (2015).

351

352 *Figure 6*

353

354 The 186 surging glaciers cover a total area of ~2670 km² (with ~110 km² variability due to the surges). Eight of
355 them (~5%) are smaller than 1 km² covering an area of ~7 km², whereas 38% are larger than 10 km² covering an
356 area of 2170 km² (or 81%) (Table 3). Garmo Glacier main trunk (80) is the largest surging glacier (83 km²) and
357 the largest non-surging glacier is Fedchenko. It is a huge dendritic valley glacier with a size of ~580 km² (without
358 the surging Bivachny tributary) and is covering 6% of the total glacier area. The region is thus dominated by the
359 vast size of Fedchenko Glacier with impacts on size-related distributions.

360

361 *Table 3*

362 The created inventories have a different count of entries due to different glacier states and topologic relations.
363 The generalised statistics for the sample with observed surges refer to the GI-3 inventory with 186 entries, whilst
364 statistics for GI-3min and GI-3max have different numbers. Compared to the full sample of glaciers in GI-2
365 (13495), surging glaciers constitute 77% by number and 80% by area in the area class 50-100 km² (Fig. 7). They
366 are also dominating the size classes 10-50 and 100-500 km² (51% and 63% by area, respectively). When
367 considering all three size classes from 10 to 500 km², two thirds of the glaciers have surged in the observation
368 period, i.e. they are the rule rather than the exception. The 22 largest surging glaciers cover almost about the same
369 area (1338 km²) ~~than as~~ the 163 smaller ones (1332 km²).

370

371 *Figure 7*

372

373 The frequency distribution of aspect sectors of surging glaciers is only slightly different from all other glaciers
374 (Fig. 8a). Surging glaciers exposed to SW contribute almost 10% ~~to~~ of the sample, whereas only 3% of the other
375 glaciers are facing in this direction. The same applies to the area covered (Fig. 8b), where surging glaciers
376 cumulate ~370 km² and thus ¼ more area than the other glaciers (~300 km²) in this sector. On the other hand, the
377 latter have higher percentages facing N and NE. The strong difference towards the N is mainly driven by
378 Fedchenko Glacier.

379

380 *Figure 8*

381

382 The scatter plot showing median elevation vs. mean aspect (Fig. 9) reveals that ~~mean~~ median elevations cover a
383 wide range of values (from about 3500 to 6000 m) and that there is some dependence on aspect, i.e. glaciers
384 facing south have a few hundred metres higher ~~mean~~ median elevations. The surging glaciers largely follow
385 ~~the~~ this distribution, but have somewhat higher elevations in the southern and lower values in the northern aspect
386 ranges compared to the other glaciers when considering ~~mean~~ median values per sector. On average, the median
387 elevation of surging glaciers is 4800 m a.s.l.

388

389 *Figure 9*

390

391 Median glacier elevations increase from west to east and show a small decrease in the most eastern and northern
392 ranges (Pamir Alai) towards the outer glaciers (Fig. 10). The marked surging glaciers are mostly found along the
393 outer boundary of the study region with generally lower median elevations. The near absence of surging glaciers
394 in the inner Pamir with its generally higher median elevations is noteworthy. However, in the Mustagh region,
395 glaciers with observed surges have the highest (5646 m) and surging glaciers in the ‘Petr Alervogo west’ region
396 the lowest values (3429 m).

397

398 *Figure 10*

399

400 As surging glaciers have a bias towards larger sizes compared to all other glaciers (see Fig. 7), they also have
401 slightly higher elevation ranges (Fig. 11a) and form the upper end of the sample. However, the spread of values
402 for glaciers with a size of about 50 km² is very large, ranging from about 2000 to nearly 5000 m. The area-
403 elevation distribution in Fig. 11b displays a smaller amount of area around the mean elevation compared to all
404 other glaciers, which is likely due to the many small glaciers in these altitudes (see black circles in Fig. 10).

405

406 *Figure 11*

408 **5.2 Observed changes**

409 For a sample of 169 and 160 glaciers, we could map their minimum and maximum extent, respectively, and for
 410 148 surges we determined the surge duration which is completely within the observation period. For 15 glaciers,
 411 we observed a full surge cycle with the onset of the next surge and for six glaciers (Bivachny 63, Dzerzhinsky
 412 104, Medvezhy 29, Right Dustiroz 31, Yazgulemdara 35, ~~OID~~ObjectID 1) two or more surges were observed
 413 over the study period. Both, the timing of the surges and their durations are highly variable (Fig. 12). Moreover,
 414 one has to consider that several glaciers (>30) were already surging on the first available Landsat TM images (in
 415 1988) and several (>20) are still surging in 2017/2018. For both cases the surge duration could not be fully
 416 determined and is thus longer than the values presented here.

417

418 *Figure 12*

419

420 The two histograms in Fig. 13 display a counting of the surges that started in a particular period (Fig. 13a) and of
 421 the surge durations in 4-year bins (Fig. 13b). For ~~both graphs~~Fig. 13a it has to be considered that the first period
 422 (1988/89) is including ~~all only~~ glaciers that ~~are already started~~ surging ~~at that time. This gives a much higher~~
 423 ~~number of surges (66) compared to those that have only started~~ in 1989 ~~(27). because it is unclear in which year~~
 424 ~~the glaciers with a 1988 starting year actually started surging.~~ For the surge duration counting in Fig. 13b this
 425 means that shorter surge periods are over-represented and are indeed longer. Furthermore, the last period is not
 426 complete (i.e. surges are on-going), which has the same effect on the counting. This results in ~~possibly likely~~ too
 427 high and too low values in the first and last period, respectively. To circumvent this bias, we have also counted
 428 all surges that took fully place within the period, i.e. started after 1989 and ended before 2017 (~~black~~grey bars in
 429 Fig. 13b). This sample is now smaller, but has still a reasonable ~~amount~~number of glaciers in all classes. Figure
 430 13a reveals that the number of surges that have started in the second and third period is the same and slowly
 431 declining afterwards. The surge duration counting displayed in Fig. 13b has a peak at 1-5 years and very similar
 432 numbers for the next four intervals. Only few glaciers (9) have surge durations exceeding 21 years. The
 433 combination start year and duration gives the number of glaciers that are surging in a particular year. We found a
 434 steady increase in this number from 1990 (54) to 2000 (114), with a plateau until 2008 (112) and a steady
 435 decrease afterwards (to 72 in 2018). In other words, in any year during the observation period at least 54 glaciers
 436 were actively surging in the study region, up to a maximum of 129 glaciers in 2006. This is far more than ~~we~~
 437 expected.

438

439 *Figure 13*

440

441 The simplified typology (see Section 4.2) counting presented in Table 4 reveals that 75% of all glaciers have
 442 freely advancing tongues, whereas 18% ~~only~~ connect to another glacier at least in their maximum extent. ~~The rest~~
 443 ~~are tributaries.~~ From the total sample of identified surging glaciers, 85% (~~176~~169 glaciers) are considerably
 444 advancing whereas the remaining 15% (26 ~~glaciers~~) are surging internally with none or only a minor terminus

445 advance. The latter were sometimes hard to detect and required application of additional measures (see Section
446 3). From the glaciers with a substantial terminus advance, most (49.62%) advance up to 1 km. Larger advances of
447 up to 2.5 km are found for 27.31% of the glaciers and 8.57.6% advanced more than 2.5 km (up to 6.7 km). Most
448 of the surges with a change in terminus position are situated in the central mountain ranges around Fedchenko
449 Glacier, whereas the eastern ranges are dominated by stable glaciers and internal surges (but with a high
450 variability). The strongest advance has been Oshanina Glacier (9) in the Petr Alervogo East mountain range with
451 4078 m. For this analysis, we excluded all glacier surges that were not fully covered by the observation period
452 (start before 1988, end after 2018-).
453

453

454 *Table 4*

455

456 One of the most active glaciers is Medvezhy Glacier (29) with a surge cycle of only ~10 years and an active
457 period of just 2 years (Kotlyakov et al., 2018). Further glaciers with relatively short (≤ 5 years) active phases are
458 spread all over the study region. During the active surge phase, 128 glaciers increased their area by a total of
459 ~119 km², which is 6% of their total area (GI-3min) and 4% of the total area in the GI-2 inventory. On average,
460 the minimum elevation decreased from 3954 m a.s.l. to 3793 m a.s.l., but individual glaciers are reaching to more
461 than 800 m lower elevations at their maximum extent. The change in minimum elevation due to a surge does not
462 depend on the elevation range (or size) of the glacier. This is also related to the fact that several large glaciers
463 show mostly internal surges with maybe only a small advance of the tongue. Similarly, also length changes due
464 to a surge do not depend on glacier size or length. However, it is noteworthy that some glaciers change their
465 length by about a factor of almost two (ObjectID 41).

466 **6. Discussion**

467 **6.1 Characteristics of the surging glaciers and their surges**

468 Surging glaciers dominate the area classes above 10 km², which would confirm earlier observations that surging
469 glaciers are comparably large (Barrand and Murray, 2006; Clarke et al., 1986; Mukherjee et al., 2017). However,
470 we found that they can also be smaller than 1 km², down to 0.3 km². Why such small glaciers surge, often
471 increasing their length considerably, needs to be further investigated. We also have to mention that there might be
472 even smaller glaciers that were not detected due to the coarse resolution of the satellite data, i.e. our sample is
473 somewhat biased towards larger glaciers. Whereas the aspect distribution of surging glaciers is very similar to all
474 other glaciers (Fig. 8), they seem to have lower median elevations than other glaciers when facing north and
475 higher ones when facing south (Fig. 9). We do not have a physical explanation for this and assume it might only
476 be an artefact of the sampling. Their spatial distribution, on the other hand, is more peculiar as they are mostly
477 found in the outer regions of the study site (Figs. 5 and 10). Their higher share of large elevation ranges (Fig.
478 11a) is related to their generally larger size and their hypsometry is very similar to other glaciers.

479

480 Within the period considered here, the starting dates of surges are comparably random (Fig. 12), indicating a
481 limited impact of climatic trends on the timing. The high number of surging glaciers (about 55 to max 120) in any

482 year is remarkable and can only be found in the Karakoram (Bhambri et al., 2017). Whether the constant increase
483 ~~(decline)~~ before the year 2000 ~~(and decline after 2008)~~ is an artefact of the sampling or has other reasons needs to
484 be investigated in a further study. A comparable increase in glacier surge activity after 1990 was also found in the
485 Karakoram by (Copland et al., 2011). Surge durations (11 years in the mean) are as diverse as in the Karakoram
486 (Bhambri et al., 2017; Paul, 2020). However, complete surge cycles ~~are not observed for many glaciers~~ (from
487 ~~one~~the start of an active phase to the next;) are only observed for a few glaciers, so this impression is biased by
488 the observation window. Due to gaps in satellite data availability, we might have missed a few glaciers displaying
489 only (short) internal surges, so the real number of surging glaciers might be even higher and the number of
490 glaciers with a short duration of active phases higher than in our sample.

491 **6.2 Criteria to identify surges**

492 The criteria we applied to identify surges were handled ~~flexible~~flexibly to consider the wide range of surge types
493 found in the region. However, the differentiation between surging and ‘only’ advancing glaciers is sometimes
494 challenging and other interpretations are possible. The very high-resolution images as available for our study site
495 from Corona / Hexagon and Google Earth / Bing Maps did not help much in determining the timing of a surge
496 (due to the large temporal gaps), but were most helpful in confirming the surge nature of a glacier in previous and
497 recent times, respectively (Lv et al. 2019, Paul 2020). The historic images clearly reveal that many glaciers in the
498 Pamir Mountains have also surged in the 1970s, however we have not used them here to derive the timing of
499 these earlier surges as this would be a large additional exercise and the temporal density of available images
500 might not be sufficient. However, we used them to confirm additional minimum and maximum extents.

501 **6.3 Uncertainties**

502 Regarding the uncertainties of the derived topographic characteristics, one has to consider that we used the GI-1
503 basis inventory from around 2000 with a DEM (GDEMv3) from around 2008 (NASA, 2018). The DEM has local
504 artefacts, is void filled and the timing of both datasets does not match. The latter is in particular the case for
505 glaciers that surged between 2000 and 2009 and had strong changes in geometry. The strongest impact is likely
506 on minimum elevation, but also median elevation, aspect and mean slope might be impacted. There is little we
507 can do about this uncertainty, as otherwise we would need a DEM from nearly every year, synchronous with the
508 timing of the minimum glacier extent. However, for the overall statistical analysis of the datasets presented here,
509 the impact of the temporal mismatch on the graphs is likely small. Of course, when individual glaciers are
510 analysed, this mismatch has to be considered (Frey and Paul, 2012).

511
512 Regarding the timing of the observed surges, we face the following uncertainties:

513 a) We have only analysed the time window 1988 to 2018; the assigned duration of surges starting before 1988 or
514 ending after 2018 is thus too short,

515 b) we only include glaciers with an active surge phase between 1988 and 2018; the real number of glaciers in the
516 study region that surged in the past might thus be higher,

517 c) for most regions we do not have usable satellite images in every year (e.g. due to snow and clouds); this adds
518 to the uncertainty of the start/end assignment and could even result in completely missed short-lived internal
519 surges,
520 d) the spatial resolution of Landsat sometimes impacts a proper identification of the terminus, in particular when
521 debris-covered; this leads to uncertainties in the timing,
522 e) due to residual dead ice in the glacier forefield and debris cover, the timing of the minimum extent is more
523 difficult to define than the maximum; in uncertain cases we used the extent from GI-3, and
524 f) when surges start with a mass wave and/or stay internal (no terminus advance), the timing derived from visual
525 analysis will likely be different from studies analysing flow velocities.
526 Collectively, it is likely that other analysts derive different start/end dates of individual surges, but in most cases
527 the difference will not exceed a few years. This will thus not affect the overall conclusions about the highly
528 variable timing of surges and surge durations.

529

530 The ~~here presented~~ assignment of surge classes presented here should be robust as we used qualitative and
531 categorised criteria that will not change much for a different interpretation. However, not all surges of the same
532 glacier end up in the same class. For example, if a recent surge is more dynamic than a previous one, it might
533 reach another glacier and become a part-time tributary. Also internal surges might have shown advancing termini
534 before and are thus not strictly internal. Hence, the assigned classes can vary for other surges. In general, we only
535 assigned the characteristics of the surge of the main glacier trunk to the attribute table.

536 **6.4 Comparison to other inventories**

537 Compared to previous studies, we identified several new surging glaciers. Some of the probable or possible
538 (category 2 and 3) surges listed in Osipova et al. (1998) have indeed surged and are now included in our
539 inventory. Most others found in these categories could not be confirmed as the morphological details used to
540 identify surge activities are only visible in very high-resolution imagery (at least 2 m) rather than with 30 or 15 m
541 Landsat data we used here. It is, however, well possible that they surged outside our observation window.

542

543 Sevestre and Benn (2015) presented 820 possible surge-type glaciers in the Pamir mainly based on the inventory
544 by Osipova et al. (1998). Our findings are in good agreement with the 51 most reliably classified (category 3)
545 surge-type glaciers marked in the RGI (we include 45 of them). Our 132 additional surging glaciers belong
546 mostly (55 of 188) to category (2 – probably surging) in the RGI, and a few (18 of 322) belong to category (1 –
547 possibly surging). The remaining 52 surging glaciers were not indicated as surge-type in the RGI. When
548 considering the 14 further glaciers which were mentioned by Lv et al. (2019), 38 (20.5% of the total sample) so
549 far unknown surging glaciers have been identified here for the Pamir. Outlines from two of our surging glaciers
550 (ObjectIDs 65 and 64) are missing in the RGI 6.0.

551

552 Compared to Lv et al. (2019), we identified three further surging glaciers (16 in total) in the King Tau and
553 Ulugarttag sub-regions. Apart from surge-type glaciers, their study also classified four glaciers as advancing,
554 eleven as stable and one retreating. We classified one of their advancing and three of their stable glaciers as

555 surging. This new interpretation results from our longer observation period and the DEM difference images
556 revealing the typical mass redistribution patterns. The surging glaciers described by Kotlyakov et al. (2008) are in
557 full agreement with our findings. The above-mentioned numbers have to be interpreted with some care, as we
558 compared two different inventories with individual glacier divides. Thus, a direct and one-to-one comparison is
559 challenging.

560 **7. Conclusions**

561 In this study, we presented a new inventory of surging glaciers for the Pamir Mountains. The analysis is based on
562 results from earlier studies, Landsat imagery acquired over the period 1988 to 2018, the SRTM, ASTER
563 GDEMv3 and ALOS DEM₂, and declassified very-high resolution images from Corona and Hexagon- as well as
564 more recent very high-resolution satellite data (Bing Maps & Google Earth). Using animations and flicker images
565 for the Landsat time series in combination with the elevation change patterns from DEM differencing, we
566 detected 206 spatially distinct glacier surges within 186 glacier bodies. The new dataset is in good agreement
567 with previous compilations of surging glaciers and confirmed surges for 133 new glaciers that were so far only
568 marked as surge-type probable or possible. We further digitized minimum and maximum extent of 169 and 160
569 glaciers, respectively, and determined the timing for about $\frac{3}{4}$ of all surges. The temporal distribution is random
570 concerning timing and surge duration (mean value 11 years), but the high number of active surges in any year
571 (between 54 and 120) was unexpected and ~~in this amount~~ only known from previously been observed in the
572 Karakoram. The distribution of surging glaciers is biased towards the central, northern and eastern mountain
573 ranges. Their sizes range from 0.3 to 143 km² and they are dominating the size-class distribution above 10 km².
574 Three glaciers descend by more than 800 m and five increased their length by a factor of more than 2 during a
575 surge. However, advance distances are not related to original glacier length as several large glaciers only show
576 internal surges or very small advances. The three inventories created in this study (GI-3, GI-3min, GI-3max) are
577 available in the Supplemental Material to serve as a base for further investigations.

578 **8. Data availability**

579 The dataset can be downloaded from: <https://doi.pangaea.de/10.1594/PANGAEA.914150> (Goerlich et al., 2020).

580 **Author contribution**

581 F.G. and F.P. designed the study, analysed the datasets and wrote the manuscript, F.G. processed the data and
582 prepared all figures and datasets. T.B. provided additional literature and datasets. All authors contributed to the
583 writing and editing of the manuscript.

584 **Competing interests**

585 The authors declare that they have no conflict of interest.

586 **Acknowledgements**

587 The work of F.G. and F.P. was supported by the ESA projects Glaciers_cci (4000109873/14/I-NB) and
588 Glaciers_cci+ (4000127593/19/I-NB), the work of T.B. was partially supported by the Strategic Priority Research
589 Program of Chinese Academy of Sciences (XDA20100300). The AW3D30 DEM is provided by the Japan
590 Aerospace Exploration Agency (<http://www.eorc.jaxa.jp/ALOS/en/aw3d30/index.htm>) ©JAXA. All Corona,
591 Hexagon and Landsat images used in this study were provided by USGS and downloaded from
592 earthexplorer.usgs.gov. We thank P. Rastner for supporting us in calculating the topographic parameters for
593 several states of the inventory, K. Mukherjee for providing the Hexagon DEMs from 1975 and H. Machguth for
594 providing the centre lines for determination of glacier length and length changes. We thank the two anonymous
595 reviewers for their conscientious work to improve this study.

- 597 Barrand, N. E. and Murray, T.: Multivariate Controls on the Incidence of Glacier Surging in the Karakoram
598 Himalaya, Arctic, Antarct. Alp. Res., 38(4), 489–498, doi:10.1657/1523-
599 0430(2006)38[489:MCOTIO]2.0.CO;2, 2006.
- 600 Berthier, E. and Brun, F.: Karakoram geodetic glacier mass balances between 2008 and 2016: Persistence of the
601 anomaly and influence of a large rock avalanche on Siachen Glacier, *J. Glaciol.*, 65(251), 494–507,
602 doi:10.1017/jog.2019.32, 2019.
- 603 Bhambri, R., Hewitt, K., Kawishwar, P. and Pratap, B.: Surge-type and surge-modified glaciers in the
604 Karakoram, *Sci. Rep.*, 7(15391), 1–14, doi:10.1038/s41598-017-15473-8, 2017.
- 605 Bolch, T., Pieczonka, T., Mukherjee, K. and Shea, J.: Brief communication: Glaciers in the Hunza catchment
606 (Karakoram) have been nearly in balance since the 1970s, *Cryosphere*, 11(1), 531–539, doi:10.5194/tc-11-
607 531-2017, 2017.
- 608 Brun, F., Berthier, E., Wagnon, P., Kääb, A. and Treichler, D.: A spatially resolved estimate of High Mountain
609 Asia glacier mass balances from 2000 to 2016, *Nat. Geosci.*, 10(9), 668–673, doi:10.1038/ngeo2999, 2017.
- 610 Clarke, K. C., Sciamoi, P., Simon, C. and Ommanney, L.: Characteristics of Surge-Type Glaciers, *J. Geophys.*
611 *Res.*, 91(5), 7165–7180, doi:10.1029/JB091iB07p07165, 1986.
- 612 Copland, L., Sylvestre, T., Bishop, M. P., Shroder, J. F., Seong, Y. B., Owen, L. A., Bush, A. and Kamp, U.:
613 Expanded and Recently Increased Glacier Surging in the Karakoram, Arctic, Antarct. Alp. Res., 43(4), 503–
614 516, doi:10.1657/1938-4246-43.4.503, 2011.
- 615 Dolgushin, L. D. and Osipova, G. B.: New Data on the recent Glacier Surges, *Mater. Glyatsiol.*, 18, 191–217,
616 1971.
- 617 Dolgushin, L. D. and Osipova, G. B.: Glacier surges and the problem of their forecasting, *IAHS Publ.*, (104),
618 292–304, 1975.
- 619 Dowdeswell, J. A., Gorman, M. R., Macheret, Y. Y., Moskalevsky, M. Y. and Hagen, J. O.: Digital comparison
620 of high resolution Sojuzkarta KFA-1000 imagery of ice masses with Landsat and SPOT data, *Ann. Glaciol.*,
621 17, 105–112, doi:10.3189/S0260305500012684, 1993.
- 622 Dowdeswell, J. A., Glazovsky, A. F. and Macheret, Y. Y.: Ice divides and drainage basins on the ice caps of
623 Franz Josef Land, Russian High Arctic, defined from Landsat, KFA-1000, and ERS-1 SAR satellite imagery,
624 *Artic Alp. Res.*, 27(3), 264–270, doi:10.1080/00040851.1995.12003121, 1995.
- 625 Falaschi, D., Bolch, T., Lenzano, M. G., Tadono, T., Lo Vecchio, A. and Lenzano, L.: New evidence of glacier
626 surges in the Central Andes of Argentina and Chile, *Prog. Phys. Geogr.*, 42(6), 792–825,
627 doi:10.1177/0309133318803014, 2018.
- 628 Finaev, A. F., Shiyin, L., Weijia, B. and Li, J.: Climate Change And Water Potential Of The Pamir Mountains,
629 *Geogr. Environ. Sustain.*, 9(3), 88–105, doi:10.15356/2071-9388_03v09_2016_06, 2016.
- 630 Frey, H. and Paul, F.: On the suitability of the SRTM DEM and ASTER GDEM for the compilation of:
631 Topographic parameters in glacier inventories, *Int. J. Appl. Earth Obs. Geoinf.*, 18(1), 480–490,
632 doi:10.1016/j.jag.2011.09.020, 2012.
- 633 Galiatsatos, N.: The Shift from Film to Digital Product: Focus on CORONA Imagery, *Photogramm. -*
634 *Fernerkundung - Geoinf.*, 2009(3), 251–260, doi:10.1127/0935-1221/2009/0020, 2009.
- 635 Gardelle, J., Berthier, E., Arnaud, Y. and Kääb, A.: Region-wide glacier mass balances over the Pamir-
636 Karakoram-Himalaya during 1999-2011, *Cryosphere*, 7(4), 1263–1286, doi:10.5194/tc-7-1263-2013, 2013.
- 637 Goerlich, F., Bolch, T., Mukherjee, K. and Pieczonka, T.: Glacier Mass Loss during the 1960s and 1970s in the
638 Ak-Shirak Range (Kyrgyzstan) from Multiple Stereoscopic Corona and Hexagon Imagery, *Remote Sens.*,
639 9(275), doi:10.3390/rs9030275, 2017.
- 640 Goerlich, F., Bolch, T., Paul, F.: Inventory of surging glaciers in the Pamir. PANGAEA,
641 <https://doi.pangaea.de/10.1594/PANGAEA.914150>, 2020.
- 642 Herreid, S. and Truffer, M.: *Journal of Geophysical Research : Earth Surface* Automated detection of unstable
643 glacier flow and a spectrum of speedup behavior in the Alaska Range Special Section :, *J. Geophys. Res.*
644 *Earth Surf.*, 121(1), 64–81, doi:10.1002/2015JF003502.Surge-type, 2016.
- 645 Holzer, N., Golletz, T., Buchroithner, M. F. and Bolch, T.: Glacier Variations in the Trans Alai Massif and the
646 Lake Karakul Catchment (Northeastern Pamir) Measured from Space, in R.P. Singh, U. Schikhoff, & S. Mal
647 (Eds.): *Climate Change, Glacier Response, and Vegetation Dynamics in the Himalaya*, edited by R. P. Singh,
648 U. Schikhoff, and S. Mal, pp. 139–153, Springer, Cham., 2016.
- 649 Kääb, A., Isakowski, Y., Paul, F., Neumann, A. and Winter, R.: Glaziale und periglaziale Prozesse: Von der
650 statischen zur dynamischen Visualisierung, *Kartographische Nachrichten*, 53(5), 206–212, 2003.
- 651 Kotlyakov, V. M., Desinov, L. V., Osipova, G. B., Hauser, M., Tsvetkov, D. G. and Schneider, J. F.: Events in
652 2002 on Russian Geographical Society (RGO) Glacier, Pamirs, *Mater. Glyatsiol.*, 95, 221–230, 2003.

- 653 Kotlyakov, V. M., Osipova, G. B. and Tsvetkov, D. G.: Monitoring of the Pamirs surging glaciers from space,
654 *Ann. Glaciol.*, 48, 125–134, doi:10.3189/172756408784700608, 2008.
- 655 Kotlyakov, V. M., Chernova, L. P., Khromova, T. E., Muraviev, A. Y., Kachalin, A. B. and Tiufin, A. S.:
656 Unique Surges of Medvezhy Glacier, *Dokl. Earth Sci.*, 483(2), 1547–1552, doi:10.1134/s1028334x18120152,
657 2018.
- 658 Lambrecht, A., Mayer, C., Aizen, V., Floricioiu, D. and Surazakov, A.: The evolution of Fedchenko glacier in the
659 Pamir, Tajikistan, during the past eight decades, *J. Glaciol.*, 60(220), 233–244, doi:10.3189/2014JoG13J110,
660 2014.
- 661 Lambrecht, A., Mayer, C., Wendt, A., Floricioiu, D. and Völksen, C.: Elevation change of Fedchenko Glacier,
662 Pamir Mountains, from GNSS field measurements and TanDEM-X elevation models, with a focus on the
663 upper glacier, *J. Glaciol.*, 64(246), 637–648, doi:10.1017/jog.2018.52, 2018.
- 664 Liang, L., Cuo, L. and Liu, Q.: The energy and mass balance of a continental glacier: Dongkemadi Glacier in
665 central Tibetan Plateau, *Sci. Rep.*, 8(1), 1–8, doi:10.1038/s41598-018-31228-5, 2018.
- 666 Lv, M., Guo, H., Lu, X., Liu, G., Yan, S., Ruan, Z., Ding, Y. and Quincey, D. J.: Characterizing the behaviour of
667 surge- and non-surge-type glaciers in the Kingata Mountains, eastern Pamir, from 1999 to 2016, *Cryosphere*,
668 13(1), 219–236, doi:10.5194/tc-13-219-2019, 2019.
- 669 Machguth, H. and Huss, M.: The length of the world’s glaciers a new approach for the global calculation of
670 center lines, *Cryosphere*, 8(5), 1741–1755, doi:10.5194/tc-8-1741-2014, 2014.
- 671 Maussion, F., Scherer, D., Mölg, T., Collier, E., Curio, J. and Finkelnburg, R.: Precipitation seasonality and
672 variability over the Tibetan Plateau as resolved by the high Asia reanalysis, *J. Clim.*, 27(5), 1910–1927,
673 doi:10.1175/JCLI-D-13-00282.1, 2014.
- 674 Meier, M. F. and Post, A.: What are glacier surges?, *Can. J. Earth Sci.*, 6(4(2)), 807–817, 1969.
- 675 Minora, U., Bocchiola, D., D’Agata, C., Maragno, D., Mayer, C., Lambrecht, A., Vuillermoz, E., Senese, A.,
676 Compostella, C., Smiraglia, C. and Diolaiuti, G. A.: Glacier area stability in the Central Karakoram National
677 Park (Pakistan) in 2001–2010: The “Karakoram Anomaly” in the spotlight., 2016.
- 678 Mölg, N., Bolch, T., Rastner, P., Strozzi, T. and Paul, F.: A consistent glacier inventory for Karakoram and Pamir
679 derived from Landsat data: Distribution of debris cover and mapping challenges, *Earth Syst. Sci. Data*, 10(4),
680 1807–1827, doi:10.5194/essd-10-1807-2018, 2018.
- 681 Mukherjee, K., Bolch, T., Goerlich, F., Kutuzov, S., Osmonov, A., Pieczonka, T. and Shesterova, I.: Surge-type
682 glaciers in the Tien Shan (Central Asia), Arctic, *Antarct. Alp. Res.*, 49(1), 147–171,
683 doi:10.1657/AAAR0016-021, 2017.
- 684 NASA/METI/AIST/Japan Spacesystems and U.S./Japan ASTER Science Team: ASTER Global Digital
685 Elevation Model V003 [Data Set]., 2018.
- 686 Osipova, G. B., Tsvetkov, D. G., Schetinnikov, A. S. and Rudak, M. S.: Inventory of surging glaciers of the
687 Pamirs, *Mater. Glyatsiol.*, 85, 3–136, 1998.
- 688 Osipova, G. B. and Khromova, T. E.: Electronic data base “Surging glaciers of Pamir” *Ice Snow*, 50(4), 15–24,
689 2010. (in Russian)
- 690 Osipova, G. B.: Fifty years of studying the Medvezhiy Glacier (West Pamirs) by the Institute of Geography,
691 RAS, *Ice Snow*, 1, 129–140, doi:10.15356/2076-6734-2015-1-129-140, 2015.
- 692 Paul, F.: Revealing glacier flow and surge dynamics from animated satellite image sequences: Examples from the
693 Karakoram, *Cryosphere*, 9(6), 2201–2214, doi:10.5194/tc-9-2201-2015, 2015.
- 694 Paul, F.: A 60-year chronology of glacier surges in the central Karakoram from the analysis of satellite image
695 time-series, *Geomorphology*, 352, 106993, doi:10.1016/j.geomorph.2019.106993, 2020.
- 696 Paul, F., Kääb, A., Maisch, M., Kellenberger, T. and Haerberli, W.: The new remote-sensing-derived Swiss
697 glacier inventory: I. Methods, *Ann. Glaciol.*, 34, 355–361, doi:10.3189/172756402781817473, 2002.
- 698 Paul, F., Barry, R. G., Cogley, J. G., Frey, H., Haerberli, W., Ohmura, A., Ommanney, C. S. L., Raup, B., Rivera,
699 A. and Zemp, M.: Recommendations for the compilation of glacier inventory data from digital sources, *Ann.*
700 *Glaciol.*, 50(53), 119–126, doi:10.3189/172756410790595778, 2009.
- 701 Pieczonka, T., Bolch, T. and Buchroithner, M.: Generation and evaluation of multitemporal digital terrain models
702 of the Mt. Everest area from different optical sensors, *ISPRS J. Photogramm. Remote Sens.*, 66(6), 927–940,
703 doi:10.1016/j.isprsjprs.2011.07.003, 2011.
- 704 Pieczonka, T., Bolch, T., Junfeng, W. and Shiyin, L.: Heterogeneous mass loss of glaciers in the Aksu-Tarim
705 Catchment (Central Tien Shan) revealed by 1976 KH-9 Hexagon and 2009 SPOT-5 stereo imagery, *Remote*
706 *Sens. Environ.*, 130, 233–244, doi:10.1016/j.rse.2012.11.020, 2013.
- 707 Quincey, D. J., Glasser, N. F., Cook, S. J. and Luckman, A.: Heterogeneity in Karakoram glacier surges, *J.*
708 *Geophys. Res. Earth Surf.*, 120(7), 1288–1300, doi:10.1002/2015JF003515, 2015.
- 709 Rabus, B., Eineder, M., Roth, A. and Bamler, R.: The shuttle radar topography mission—a new class of digital
710 elevation models acquired by spaceborne radar, *ISPRS J. Photogramm. Remote Sens.*, 57(4), 241–262,
711 doi:10.1016/S0924-2716(02)00124-7, 2003.

- 712 Rankl, M. and Braun, M.: Glacier elevation and mass changes over the central Karakoram region estimated from
713 TanDEM-X and SRTM/X-SAR digital elevation models, *Ann. Glaciol.*, 57(71), 273–281,
714 doi:10.3189/2016AoG71A024, 2016.
- 715 Round, V., Leinss, S., Huss, M., Haemmig, C. and Hajnsek, I.: Surge dynamics and lake outbursts of Kyagar
716 Glacier, Karakoram, *Cryosphere*, 11(2), 723–739, doi:10.5194/tc-11-723-2017, 2017.
- 717 Sevestre, H. and Benn, D. I.: Climatic and geometric controls on the global distribution of surge-type glaciers:
718 Implications for a unifying model of surging, *J. Glaciol.*, 61(228), 646–662, doi:10.3189/2015JoG14J136,
719 2015.
- 720 Shean, D.: High Mountain Asia 8-meter DEM Mosaics Derived from Optical Imagery, Version, Boulder,
721 Colorado., 2017.
- 722 Steiner, J. F., Kraaijenbrink, P. D. A., Jiduc, S. G. and Immerzeel, W. W.: Brief Communication : The Khurdopin
723 glacier surge revisited – extreme flow velocities and formation of a dammed lake in 2017, *Cryosph.*, 12(1),
724 95–101, 2018.
- 725 Takaku, J., Tadono, T. and Tsutsui, K.: Generation of high resolution global DSM from ALOS PRISM, *Int. Arch.*
726 *Photogramm. Remote Sens. Spat. Inf. Sci. - ISPRS Arch.*, 40(4), 243–248, doi:10.5194/isprsarchives-XL-4-
727 243-2014, 2014.
- 728 Wendt, A., Mayer, C., Lambrecht, A. and Floricioiu, D.: A Glacier Surge of Bivachny Glacier, Pamir Mountains,
729 Observed by a Time Series of High-Resolution Digital Elevation Models and Glacier Velocities, *Remote*
730 *Sens.*, 9(4), 388, doi:10.3390/rs9040388, 2017.
- 731 Wessel, B.: TanDEM-X Ground Segment – DEM Products Specification Document”, Oberpfaffenhofen. [online]
732 Available from: <https://tandemx-science.dlr.de/>, 2016.
- 733 Yasuda, T. and Furuya, M.: Dynamics of surge-type glaciers in West Kunlun Shan, Northwestern Tibet, *J.*
734 *Geophys. Res. F Earth Surf.*, 120(11), 2393–2405, doi:10.1002/2015JF003511, 2015.
- 735 Zhang, H., Zhang, F., Zhang, G., Ma, Y., Yang, K. and Ye, M.: Daily air temperature estimation on glacier
736 surfaces in the Tibetan Plateau using MODIS LST data, *J. Glaciol.*, 64(243), 132–147,
737 doi:10.1017/jog.2018.6, 2018.
- 738
- ~~739 Berthier, E. and Brun, F.: Karakoram geodetic glacier mass balances between 2008 and 2016: Persistence of the
740 anomaly and influence of a large rock avalanche on Siachen Glacier, *J. Glaciol.*, 65(251), 494–507,
741 doi:10.1017/jog.2019.32, 2019.~~
- ~~742 Bhambri, R., Hewitt, K., Kawishwar, P. and Pratap, B.: Surge type and surge modified glaciers in the
743 Karakoram, *Sci. Rep.*, 7(15391), 1–14, doi:10.1038/s41598-017-15473-8, 2017.~~
- ~~744 Bolch, T., Pieczonka, T., Mukherjee, K. and Shea, J.: Brief communication: Glaciers in the Hunza catchment
745 (Karakoram) have been nearly in balance since the 1970s, *Cryosphere*, 11(1), 531–539, doi:10.5194/tc-11-
746 531-2017, 2017.~~
- ~~747 Brun, F., Berthier, E., Wagnon, P., Käab, A. and Treichler, D.: A spatially resolved estimate of High Mountain
748 Asia glacier mass balances from 2000 to 2016, *Nat. Geosci.*, 10(9), 668–673, doi:10.1038/ngeo2999, 2017.~~
- ~~749 Clarke, K. C., Sciiimoi, P., Simon, C. and Ommanney, L.: Characteristics of Surge Type Glaciers, *J. Geophys.*
750 *Res.*, 91(5), 7165–7180, doi:10.1029/JB091iB07p07165, 1986.~~
- ~~751 Dolgushin, L. D. and Osipova, G. B.: New Data on the recent Glacier Surges, *Mater. Glyatsiol.*, 18, 191–217,
752 1971.~~
- ~~753 Dolgushin, L. D. and Osipova, G. B.: Glacier surges and the problem of their forecasting, *IAHS Publ.*, (104),
754 292–304, 1975.~~
- ~~755 Dowdeswell, J. A., Gorman, M. R., Macheret, Y. Y., Moskalevsky, M. Y. and Hagen, J. O.: Digital comparison
756 of high resolution Sojuzkarta KFA-1000 imagery of ice masses with Landsat and SPOT data, *Ann. Glaciol.*,
757 17, 105–112, doi:10.3189/S0260305500012684, 1993.~~
- ~~758 Dowdeswell, J. A., Glazovsky, A. F. and Macheret, Y. Y.: Ice divides and drainage basins on the ice caps of
759 Franz Josef Land, Russian High Arctic, defined from Landsat, KFA-1000, and ERS-1 SAR satellite imagery,
760 *Artic Alp. Res.*, 27(3), 264–270, doi:10.1080/00040851.1995.12003121, 1995.~~
- ~~761 Falaschi, D., Bolch, T., Lenzano, M. G., Tadono, T., Lo Vecchio, A. and Lenzano, L.: New evidence of glacier
762 surges in the Central Andes of Argentina and Chile, *Prog. Phys. Geogr.*, 42(6), 792–825,
763 doi:10.1177/0309133318803014, 2018.~~
- ~~764 Finaev, A. F., Shiyin, L., Weijia, B. and Li, J.: Climate Change And Water Potential Of The Pamir Mountains,
765 *Geogr. Environ. Sustain.*, 9(3), 88–105, doi:10.15356/2071-9388_03v09_2016_06, 2016.~~
- ~~766 Frey, H. and Paul, F.: On the suitability of the SRTM DEM and ASTER GDEM for the compilation of:
767 Topographic parameters in glacier inventories, *Int. J. Appl. Earth Obs. Geoinf.*, 18(1), 480–490,
768 doi:10.1016/j.jag.2011.09.020, 2012.~~
- ~~769 Galiatsatos, N.: The Shift from Film to Digital Product: Focus on CORONA Imagery, *Photogramm.—
770 Fernerkundung Geoinf.*, 2009(3), 251–260, doi:10.1127/0935-1221/2009/0020, 2009.~~

- 771 Gardelle, J., Berthier, E., Arnaud, Y. and Kääh, A.: Region-wide glacier mass balances over the Pamir-
772 Karakoram Himalaya during 1999–2011, *Cryosphere*, 7(4), 1263–1286, doi:10.5194/te-7-1263-2013, 2013.
- 773 Goerlich, F., Bolch, T., Mukherjee, K. and Pieczonka, T.: Glacier Mass Loss during the 1960s and 1970s in the
774 Ak-Shirak Range (Kyrgyzstan) from Multiple Stereoscopic Corona and Hexagon Imagery, *Remote Sens.*,
775 9(275), doi:10.3390/rs9030275, 2017.
- 776 Goerlich, F., Bolch, T., Paul, F.: Inventory of surging glaciers in the Pamir. PANGAEA, , 2020.
- 777 Herreid, S. and Truffer, M.: Journal of Geophysical Research: Earth Surface Automated detection of unstable
778 glacier flow and a spectrum of speedup behavior in the Alaska Range Special Section :, *J. Geophys. Res.*
779 *Earth Surf.*, 121(1), 64–81, doi:10.1002/2015JF003502.Surge-type, 2016.
- 780 Holzer, N., Golletz, T., Buchroithner, M. F. and Bolch, T.: Glacier Variations in the Trans-Alai Massif and the
781 Lake Karakul Catchment (Northeastern Pamir) Measured from Space, in R.P. Singh, U. Schikhoff, & S. Mal
782 (Eds.): *Climate Change, Glacier Response, and Vegetation Dynamics in the Himalaya*, edited by R. P. Singh,
783 U. Schikhoff, and S. Mal, pp. 139–153, Springer, Cham., 2016.
- 784 Kääh, A., Isakowski, Y., Paul, F., Neumann, A. and Winter, R.: Glaziale und periglaziale Prozesse: Von der
785 statischen zur dynamischen Visualisierung, *Kartographische Nachrichten*, 53(5), 206–212, 2003.
- 786 Kotlyakov, V. M., Desinov, L. V., Osipova, G. B., Hauser, M., Tsvetkov, D. G. and Schneider, J. F.: Events in
787 2002 on Russian Geographical Society (RGO) Glacier, Pamirs, *Mater. Glyatsiol.*, 95, 221–230, 2003.
- 788 Kotlyakov, V. M., Osipova, G. B. and Tsvetkov, D. G.: Monitoring of the Pamirs surging glaciers from space,
789 *Ann. Glaciol.*, 48, 125–134, doi:10.3189/172756408784700608, 2008.
- 790 Kotlyakov, V. M., Chernova, L. P., Khromova, T. E., Muraviev, A. Y., Kachalin, A. B. and Tiuflin, A. S.:
791 Unique Surges of Medvezhy Glacier, *Dokl. Earth Sci.*, 483(2), 1547–1552, doi:10.1134/s1028334x18120152,
792 2018.
- 793 Lambrecht, A., Mayer, C., Aizen, V., Floricioiu, D. and Surazakov, A.: The evolution of Fedchenko glacier in the
794 Pamir, Tajikistan, during the past eight decades, *J. Glaciol.*, 60(220), 233–244, doi:10.3189/2014JoG13J110,
795 2014.
- 796 Lambrecht, A., Mayer, C., Wendt, A., Floricioiu, D. and Völksen, C.: Elevation change of Fedchenko Glacier,
797 Pamir Mountains, from GNSS field measurements and TanDEM-X elevation models, with a focus on the
798 upper glacier, *J. Glaciol.*, 64(246), 637–648, doi:10.1017/jog.2018.52, 2018.
- 799 Liang, L., Cuo, L. and Liu, Q.: The energy and mass balance of a continental glacier: Dongkemadi Glacier in
800 central Tibetan Plateau, *Sci. Rep.*, 8(1), 1–8, doi:10.1038/s41598-018-31228-5, 2018.
- 801 Lv, M., Guo, H., Lu, X., Liu, G., Yan, S., Ruan, Z., Ding, Y. and Quincey, D. J.: Characterizing the behaviour of
802 surge and non-surge type glaciers in the Kingata Mountains, eastern Pamir, from 1999 to 2016, *Cryosphere*,
803 13(1), 219–236, doi:10.5194/te-13-219-2019, 2019.
- 804 Machguth, H. and Huss, M.: The length of the world's glaciers—a new approach for the global calculation of
805 center lines, *Cryosphere*, 8(5), 1741–1755, doi:10.5194/te-8-1741-2014, 2014.
- 806 Maussion, F., Scherer, D., Mölg, T., Collier, E., Curio, J. and Finkelnburg, R.: Precipitation seasonality and
807 variability over the Tibetan Plateau as resolved by the high Asia reanalysis, *J. Clim.*, 27(5), 1910–1927,
808 doi:10.1175/JCLI-D-13-00282.1, 2014.
- 809 Minora, U., Bocchiola, D., D'Agata, C., Maragno, D., Mayer, C., Lambrecht, A., Vuillermoz, E., Senese, A.,
810 Compostella, C., Smiraglia, C. and Diolaiuti, G. A.: Glacier area stability in the Central Karakoram National
811 Park (Pakistan) in 2001–2010: The “Karakoram Anomaly” in the spotlight., 2016.
- 812 Mölg, N., Bolch, T., Rastner, P., Strozzi, T. and Paul, F.: A consistent glacier inventory for Karakoram and Pamir
813 derived from Landsat data: Distribution of debris cover and mapping challenges, *Earth Syst. Sci. Data*, 10(4),
814 1807–1827, doi:10.5194/essd-10-1807-2018, 2018.
- 815 Mukherjee, K., Bolch, T., Goerlich, F., Kutuzov, S., Osmonov, A., Pieczonka, T. and Shesterova, I.: Surge-type
816 glaciers in the Tien-Shan (Central Asia), *Arctic, Antarctic, Alp. Res.*, 49(1), 147–171,
817 doi:10.1657/AAAR0016-021, 2017.
- 818 NASA/METI/AIST/Japan Spacesystems, and U.S./Japan ASTER Science Team: ASTER Global Digital
819 Elevation Model V003, distributed by NASA EOSDIS Land Processes DAAC,
820 <https://doi.org/10.5067/ASTER/ASTGTM.003>, 2018.
- 821 Osipova, G. B.: Fifty years of studying the Medvezhiy Glacier (West Pamirs) by the Institute of Geography,
822 RAS, *Ice Snow*, 1, 129–140, doi:10.15356/2076-6734-2015-1-129-140, 2015. (in Russian)
- 823 Osipova, G. B. and Khromova, T. E.: Electronic data base “Surging glaciers of Pamir” *Ice Snow*, 50(4), 15–24,
824 2010. (in Russian)
- 825 Osipova, G. B., Tsvetkov, D. G., Schetinnikov, A. S. and Rudak, M. S.: Inventory of surging glaciers of the
826 Pamirs, *Mater. Glyatsiol.*, 85, 3–136, 1998. (in Russian)
- 827 Paul, F., Kääh, A., Maisch, M., Kellenberger, T. and Haerberli, W.: The new remote sensing-derived Swiss
828 glacier inventory: I. Methods, *Ann. Glaciol.*, 34, 355–361, doi:10.3189/172756402781817473, 2002.
- 829 Paul, F., Barry, R. G., Cogley, J. G., Frey, H., Haerberli, W., Ohmura, A., Ommanney, C. S. L., Raup, B., Rivera,

830 A. and Zemp, M.: Recommendations for the compilation of glacier inventory data from digital sources, *Ann.*
831 *Glaciol.*, 50(53), 119–126, doi:10.3189/172756410790595778, 2009.

832 Paul, F.: Revealing glacier flow and surge dynamics from animated satellite image sequences: Examples from the
833 Karakoram, *Cryosphere*, 9(6), 2201–2214, doi:10.5194/te-9-2201-2015, 2015.

834 Paul, F.: A 60-year chronology of glacier surges in the central Karakoram from the analysis of satellite image
835 time-series, *Geomorphology*, 352, 106993, doi:10.1016/j.geomorph.2019.106993, 2020.

836 Pieczonka, T., Boleh, T. and Buchroithner, M.: Generation and evaluation of multitemporal digital terrain models
837 of the Mt. Everest area from different optical sensors, *ISPRS J. Photogramm. Remote Sens.*, 66(6), 927–940,
838 doi:10.1016/j.isprsjprs.2011.07.003, 2011.

839 Pieczonka, T., Boleh, T., Junfeng, W. and Shiyin, L.: Heterogeneous mass loss of glaciers in the Aksu-Tarim
840 Catchment (Central Tien Shan) revealed by 1976 KH-9 Hexagon and 2009 SPOT-5 stereo imagery, *Remote*
841 *Sens. Environ.*, 130, 233–244, doi:10.1016/j.rse.2012.11.020, 2013.

842 Quincey, D. J., Glasser, N. F., Cook, S. J. and Luckman, A.: Heterogeneity in Karakoram glacier surges, *J.*
843 *Geophys. Res. Earth Surf.*, 120(7), 1288–1300, doi:10.1002/2015JF003515, 2015.

844 Rabus, B., Eineder, M., Roth, A. and Bamler, R.: The shuttle radar topography mission—a new class of digital
845 elevation models acquired by spaceborne radar, *ISPRS J. Photogramm. Remote Sens.*, 57(4), 241–262,
846 doi:10.1016/S0924-2716(02)00124-7, 2003.

847 Rankl, M. and Braun, M.: Glacier elevation and mass changes over the central Karakoram region estimated from
848 TanDEM-X and SRTM/X-SAR digital elevation models, *Ann. Glaciol.*, 57(71), 273–281,
849 doi:10.3189/2016AoG71A024, 2016.

850 Round, V., Leinss, S., Huss, M., Haemmig, C. and Hajsek, I.: Surge dynamics and lake outbursts of Kyagar
851 Glacier, Karakoram, *Cryosphere*, 11(2), 723–739, doi:10.5194/te-11-723-2017, 2017.

852 Sevestre, H. and Benn, D. I.: Climatic and geometric controls on the global distribution of surge-type glaciers:
853 Implications for a unifying model of surging, *J. Glaciol.*, 61(228), 646–662, doi:10.3189/2015JoG14J136,
854 2015.

855 Shean, D.: High Mountain Asia 8-meter DEM Mosaics Derived from Optical Imagery, Version, Boulder,
856 Colorado., 2017.

857 Steiner, J. F., Kraaijenbrink, P. D. A., Jiduc, S. G. and Immerzeel, W. W.: Brief Communication: The Khurdopin
858 glacier surge revisited—extreme flow velocities and formation of a dammed lake in 2017, *Cryosph.*, 12(1),
859 95–101, 2018.

860 Tachikawa, T., Hato, M., Kaku, M. and Iwasaki, A.: Characteristics of ASTER GDEM version 2, Vancouver,
861 BC., 2011.

862 Takaku, J., Tadono, T. and Tsutsui, K.: Generation of high-resolution global DSM from ALOS PRISM, *Int. Arch.*
863 *Photogramm. Remote Sens. Spat. Inf. Sci. ISPRS Arch.*, 40(4), 243–248, doi:10.5194/isprarchives-XL-4-
864 243-2014, 2014.

865 Wendt, A., Mayer, C., Lambrecht, A. and Floricioiu, D.: A Glacier Surge of Bivachny Glacier, Pamir Mountains,
866 Observed by a Time Series of High-Resolution Digital Elevation Models and Glacier Velocities, *Remote*
867 *Sens.*, 9(4), 388, doi:10.3390/rs9040388, 2017.

868 Wessel, B.: TanDEM-X Ground Segment—DEM Products Specification Document”, Oberpfaffenhofen. [online]
869 Available from: <https://tandemx-science.dlr.de/>, 2016.

870 Yasuda, T. and Furuya, M.: Dynamics of surge-type glaciers in West Kunlun Shan, Northwestern Tibet, *J.*
871 *Geophys. Res. Earth Surf.*, 120(11), 2393–2405, doi:10.1002/2015JF003511, 2015.

872 Zhang, H., Zhang, F., Zhang, G., Ma, Y., Yang, K. and Ye, M.: Daily air temperature estimation on glacier
873 surfaces in the Tibetan Plateau using MODIS LST data, *J. Glaciol.*, 64(243), 132–147,
874 doi:10.1017/jog.2018.6, 2018.

875

876 **Tables**

877

878 *Table 1: Main characteristics of the satellite scenes used (see Table S1 for scene list).*

Satellite	Sensor	Resolution	Period	Purpose
Corona	KH-4	2-5 m	1968	DEM generation, high-res. info
Hexagon	KH-9	5-10 m	1975/1980	Additional DEM and high-res. info
Landsat	MSS	60 m	1972-1980	Extension back in time
Landsat	TM	30 m	1989-2012	Animation
Landsat	ETM+	30 m	1999-2018	Animation
Landsat	OLI	30 m	2013-2018	Animation

879

880

881 *Table 2: Selected characteristics of available DEMs and their usage in this study.*

DEM	Type	Sensor	Resolution	Acquisition period	Date of tiles?	Usage
GDEMv3	optical	ASTER	30 m	2000-2013	No	Heights for Corona, topographic parameters
SRTM	SAR-C	SRTM	30 m	Feb 2000	Yes	Elevation changes
ALOS	optical	PRISM	30 m	2007-2011	No	elevation changes 2000 to 2009
TDX	SAR-X	TanDEM-X	90 m	2012-2015	No	Elevation changes ~2009 to ~2014
Corona	optical	KH4-B	15 m	1968	Yes	Elevation changes 1968 to 2000; Orthophoto

882

883 *Table 3: Size class distribution of surging glaciers and other glaciers of GI-2 and GI-3.*

Size Class km ²		<0.05	0.05	0.1	0.5	1	5	10	50	100	>500
			-	-	-	-	-	-	-	-	
			0.1	0.5	1	5	10	50	100	500	
other glaciers	km ²	103.7	154.7	1104	1090.7	3353.4	1172.7	1190.1	167.8	154	580.3
	%	1.1	1.7	12.2	12	37	12.9	13.1	1.9	1.7	6.4
surging glaciers	km ²	0	0	0.4	6.1	174.2	319.7	1229	682.9	262.6	0
	%	0	0	0	0.2	6.5	12	46	25.5	9.8	0
all glaciers	km ²	103.7	154.7	1104.5	1096.9	3527.6	1492.3	2419.2	850.6	416.6	580.3
	%	0.9	1.3	9.4	9.3	30	12.7	20.6	7.2	3.5	4.9
Surging proportion in %		0	0	0	0	0	21.4	50.8	80.3	63	0

884

885

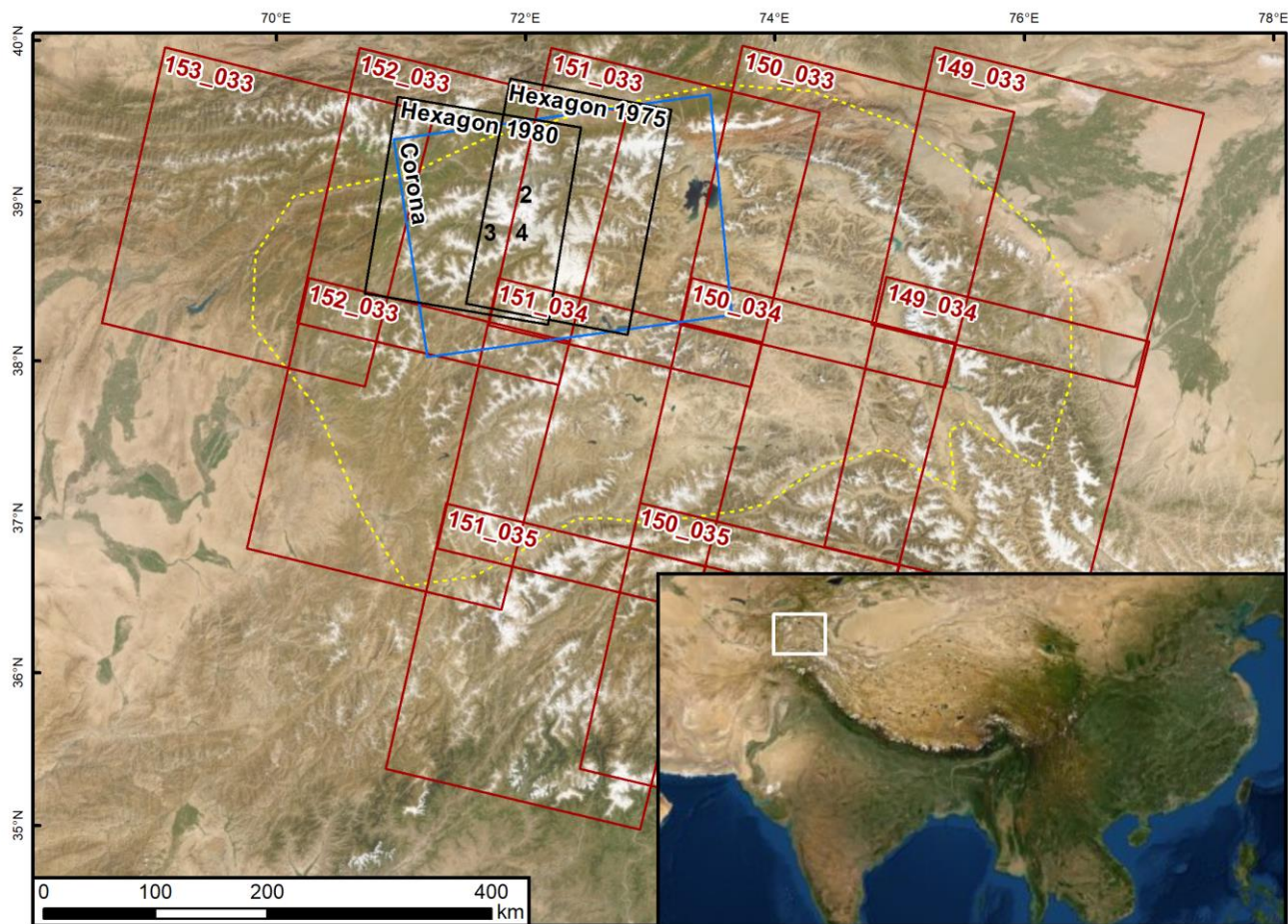
886 *Table 4: Results of the surging classification (counting per class). Glaciers with incomplete active surge phases (starting before 1988 or ending after 2018 and marked with a "0" for the distance criterion) are not listed here.*887 *(starting before 1988 or ending after 2018 and marked with a "0" for the distance criterion) are not listed here.*888 *See Section 4.2 for the meaning of classes 1, 2, and 3.*

Criteria	1	2	3	Total
Tongue	150	32	16	198
Type	169	25	4	198
Duration	21	63	114	198
Distance	106	53	13	172

889

890

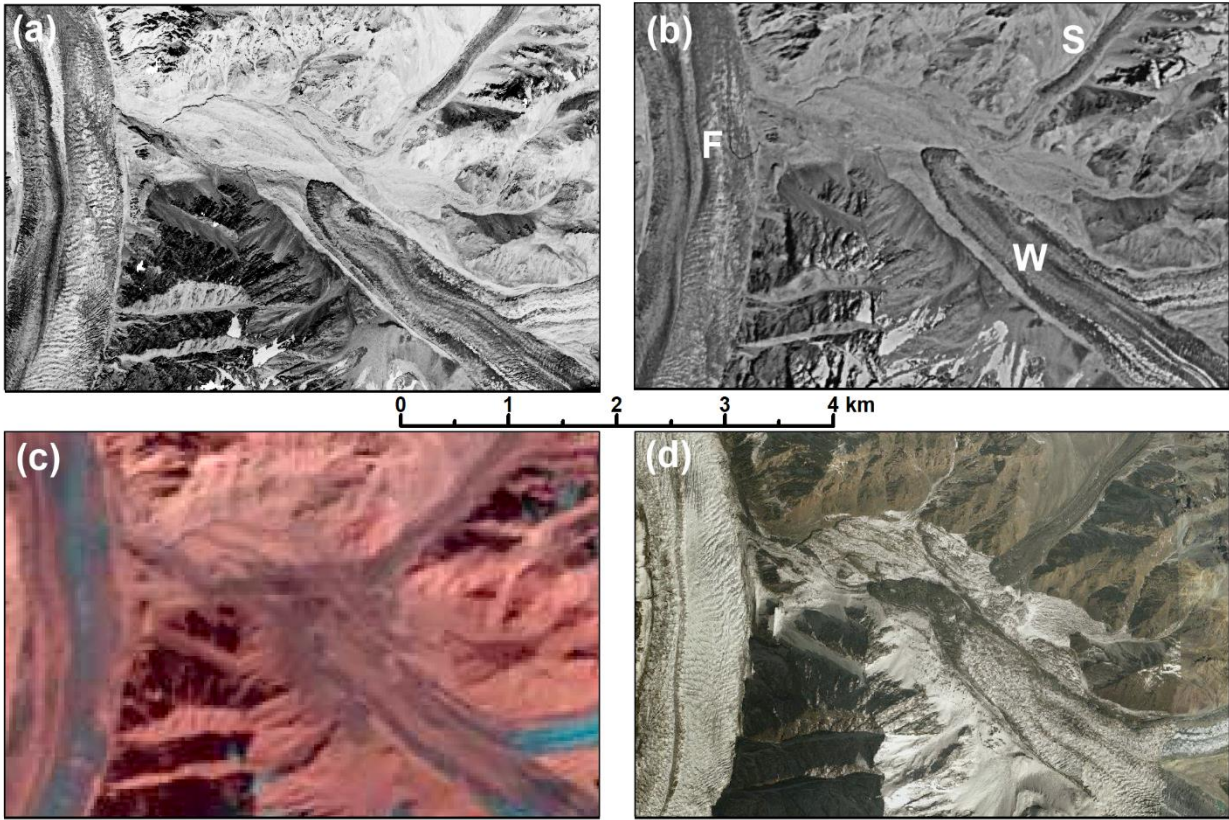
892



893

894 *Fig. 1: Location of the study region (white square in the inset) and footprints of the Corona (blue), Hexagon*
 895 *(black) and Landsat (red) scenes used in this study. The dashed yellow line marks the perimeter of the study*
 896 *region. The location of the sub-regions displayed in Figs. 2, 3 and 4 are marked with their respective numbers.*
 897 *Image sources: screenshots from © Google Earth.*

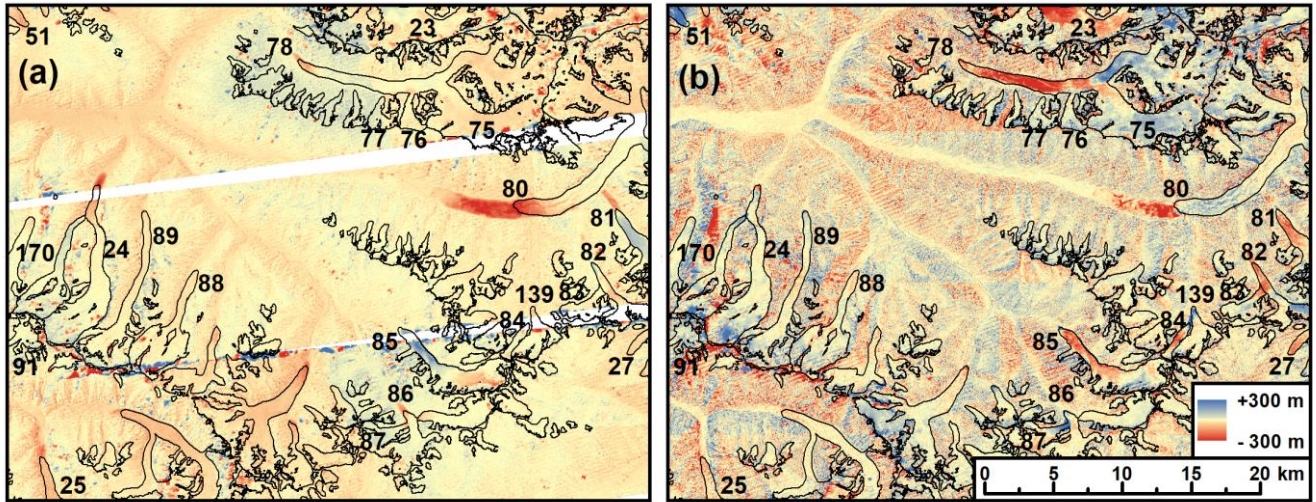
898



899

900 *Fig. 2: Comparison of satellite images for the same sub-region (see Fig. 1 for location) showing the following*
 901 *glaciers: F: Fortambek (18), W: Walter 731 (19), and S: Soldatov (20). The images are acquired by a) Corona in*
 902 *1968, b) Hexagon in 1975, c) Landsat in 2017, and d) Bing Maps (date unknown). Image sources: Panels a) to c)*
 903 *earthexplorer.usgs.gov, panel d) screenshot from bing.com ©2020 DigitalGlobe.*

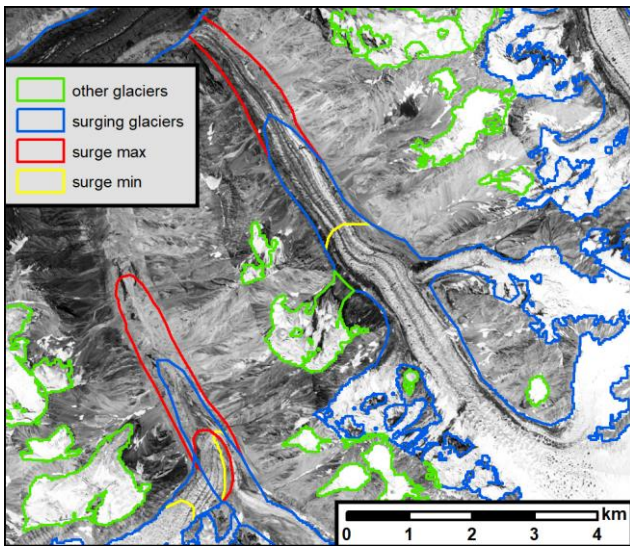
904



905

906 *Fig. 3: Two examples of colour-coded DEM difference images used to identify surging glaciers (marked with*
 907 *their ObjectID). The glacier outlines depict the glacier state ~~at~~in ~2000 (GI-2). A) SRTM-Corona (2000-1968)*
 908 *and b) AW3D30-SRTM (~2010-2000).*

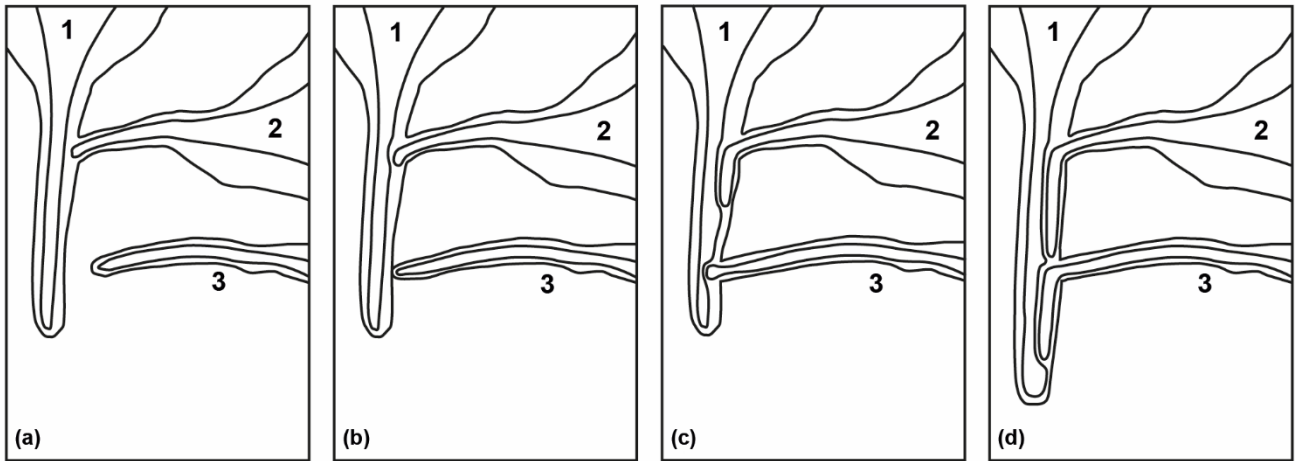
909



910

911 *Fig. 4: Comparison of glacier outlines from the original inventory GI-2 (blue/green)*
 912 */ GI-3max (yellow/red) showing the minimum and maximum extents of two surging glaciers.*
 913 *Image acquisition date and source: 1968, earthexplorer.usgs.gov.*

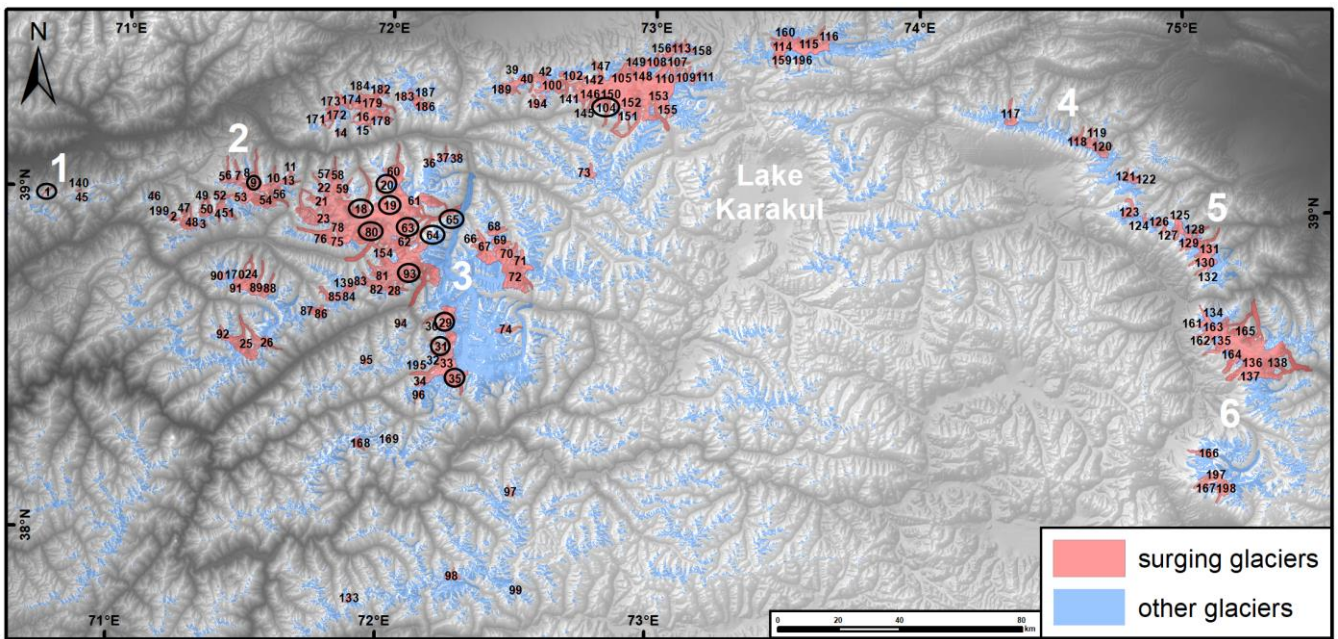
914



915

916 *Fig. 5: Sketch map of selected possible interactions among surging glaciers of different types.*
 917 *a) At the beginning – glacier 2 in full surge mode, b) surge maximum of glacier 2 and surge start of glacier 3,*
 918 *c) surge maximum of glacier 3, d) surge of glacier 1. See text for description.*

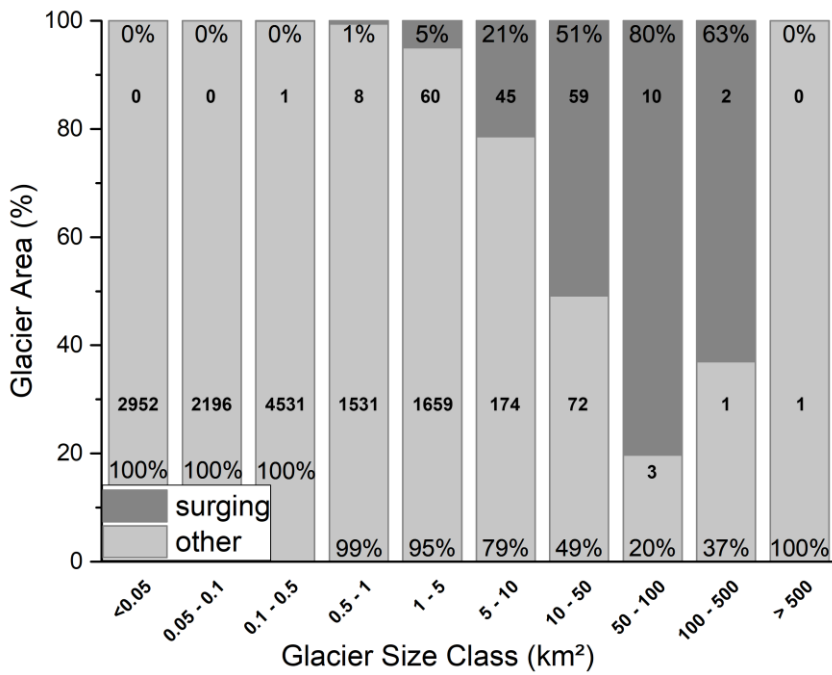
919



920

921 *Fig. 6: Overview of the identified surging glaciers (red) in the Pamir Mountains. Small black numbers refer to*
 922 *their ObjectID in the GI-3min dataset, numbers in circles indicate glaciers mentioned in the text and bold white*
 923 *numbers indicate regions mentioned in the text (1 Petr Alervogo West, 2 Petr Alervogo East, 3 Fedchenko, 4*
 924 *King Tau, 5 Ulugartag, 6 Mustagh). DEM source: AW3D30.*

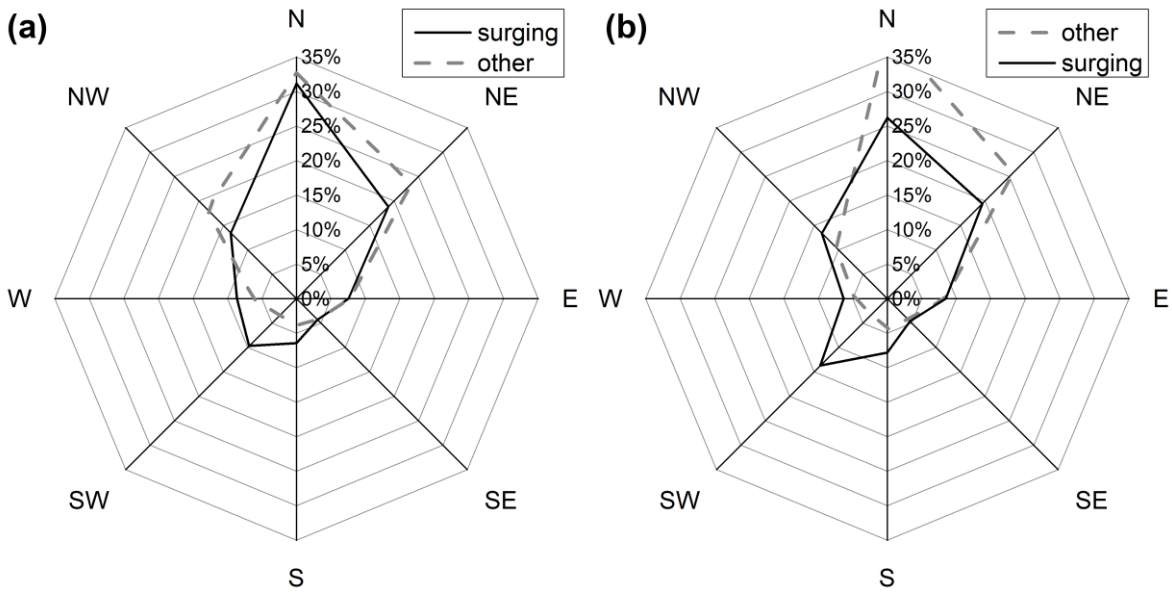
925



926

927 *Fig. 7: Size class distribution (in relative terms) of surging and other glaciers in GI-2. The upper bold numbers*
 928 *provide the count for surge glaciers, the lower one for all other glaciers.*

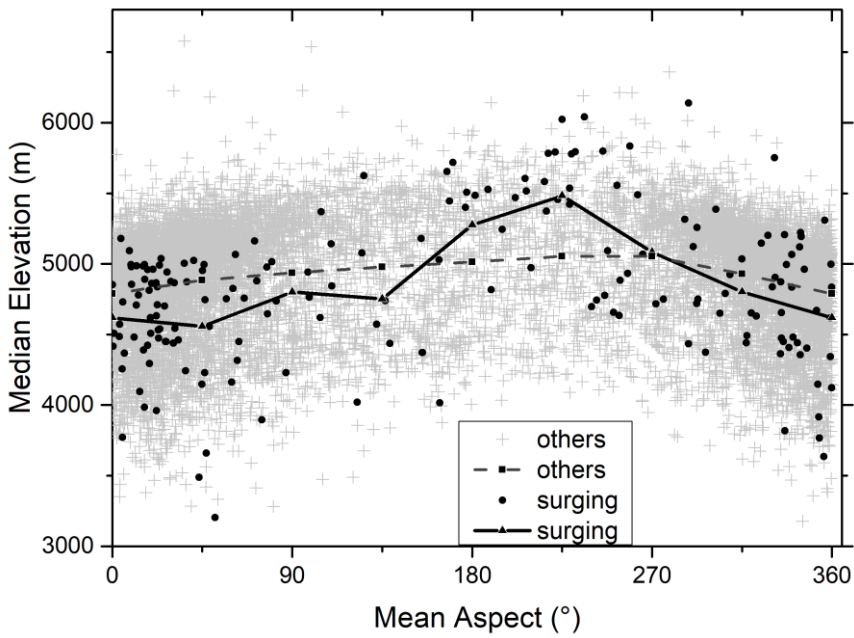
929



930

931 *Fig. 8: Aspect sector distribution for surging and other glaciers (in relative terms) per a) count and b) area*
 932 *covered.*

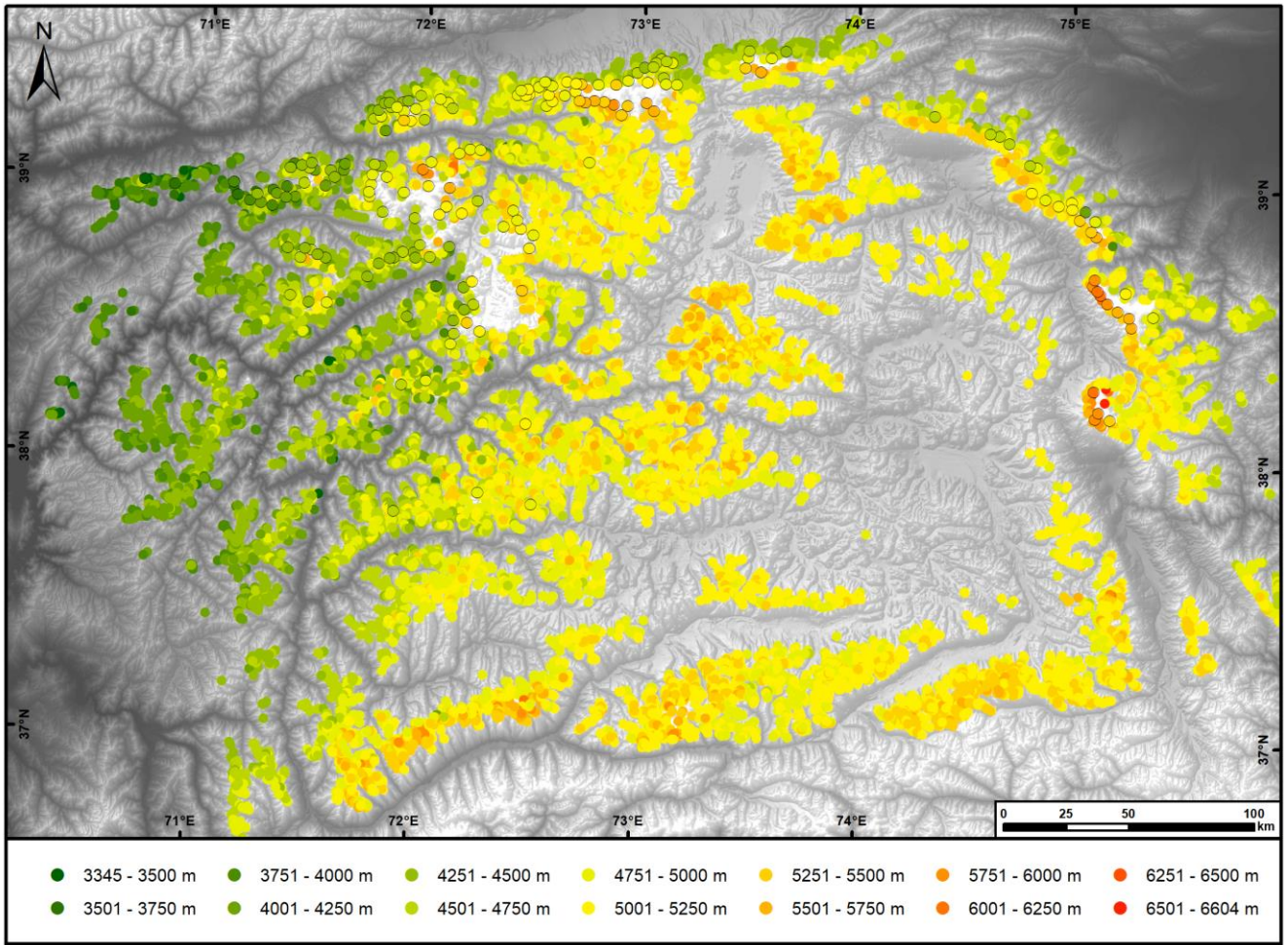
933



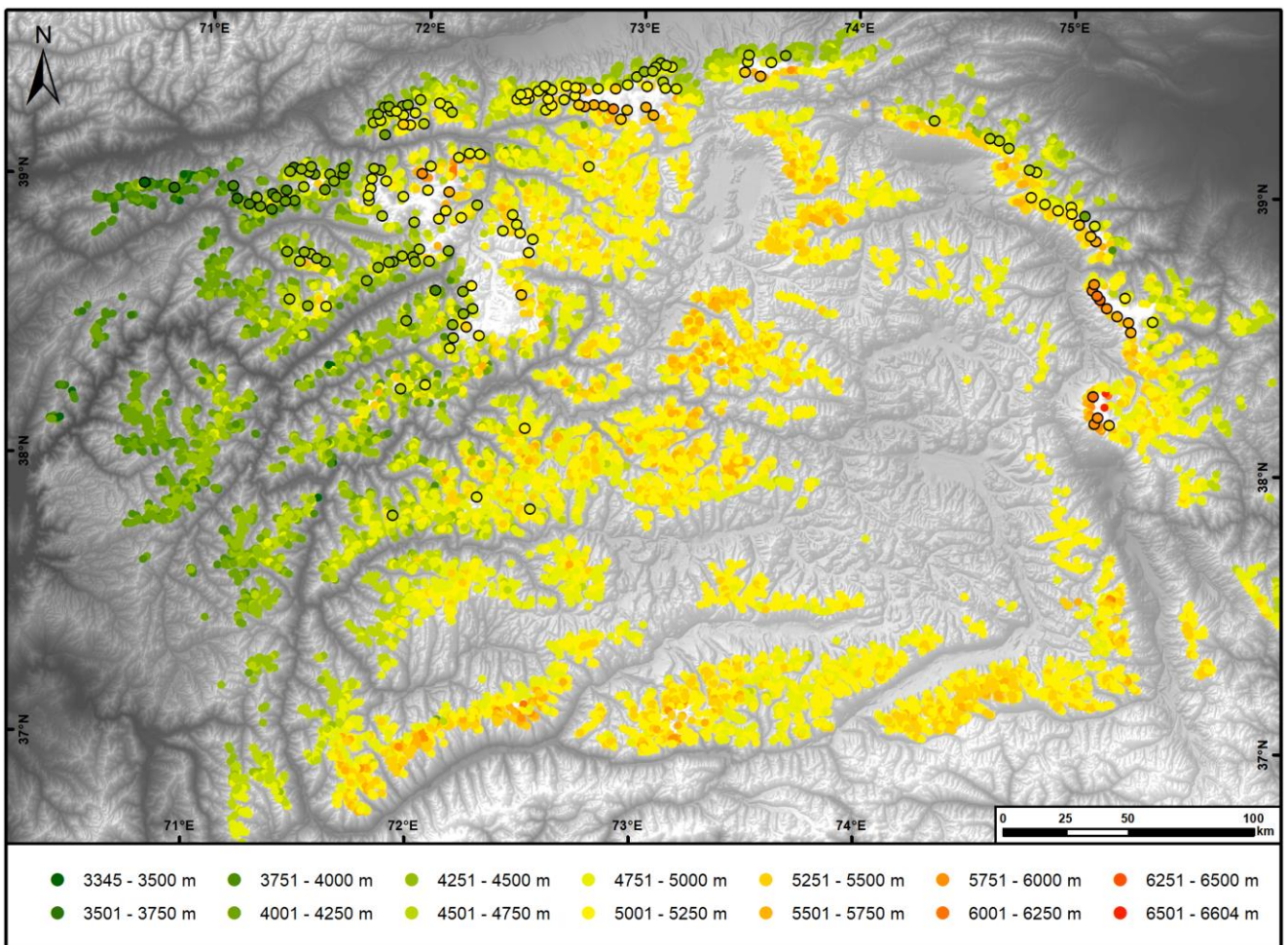
934

935 *Fig. 9: Mean aspect vs. median glacier elevation for surging and other glaciers. The connected lines are*
 936 *averages per aspect sector.*

937



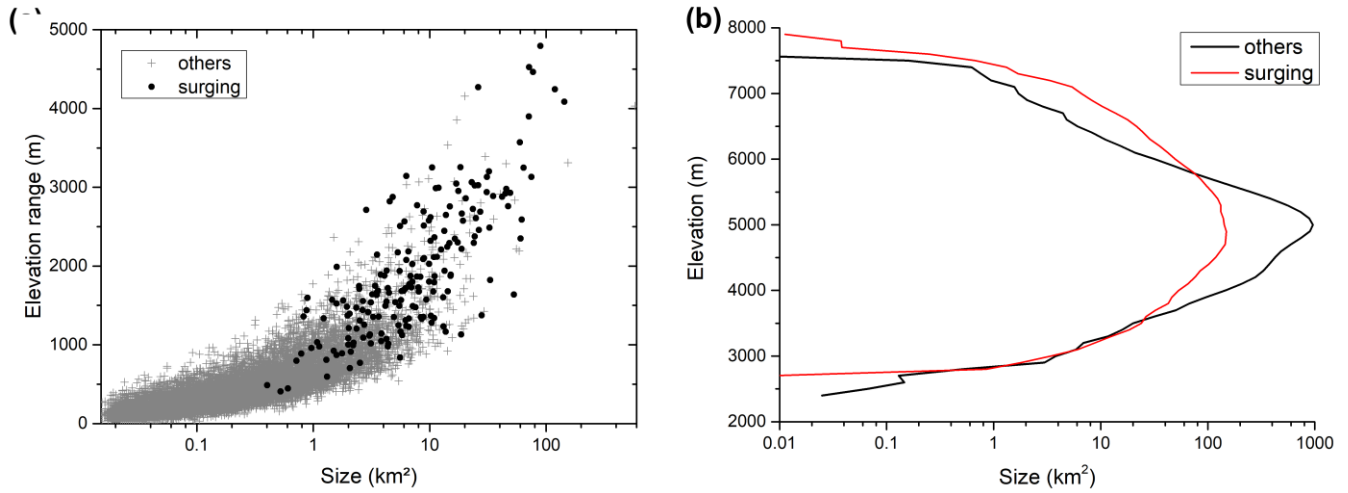
938



939

940 Fig. 10: Colour-coded median elevation map with surging glaciers marked (circles with outlines). DEM
941 source: AW3D30.

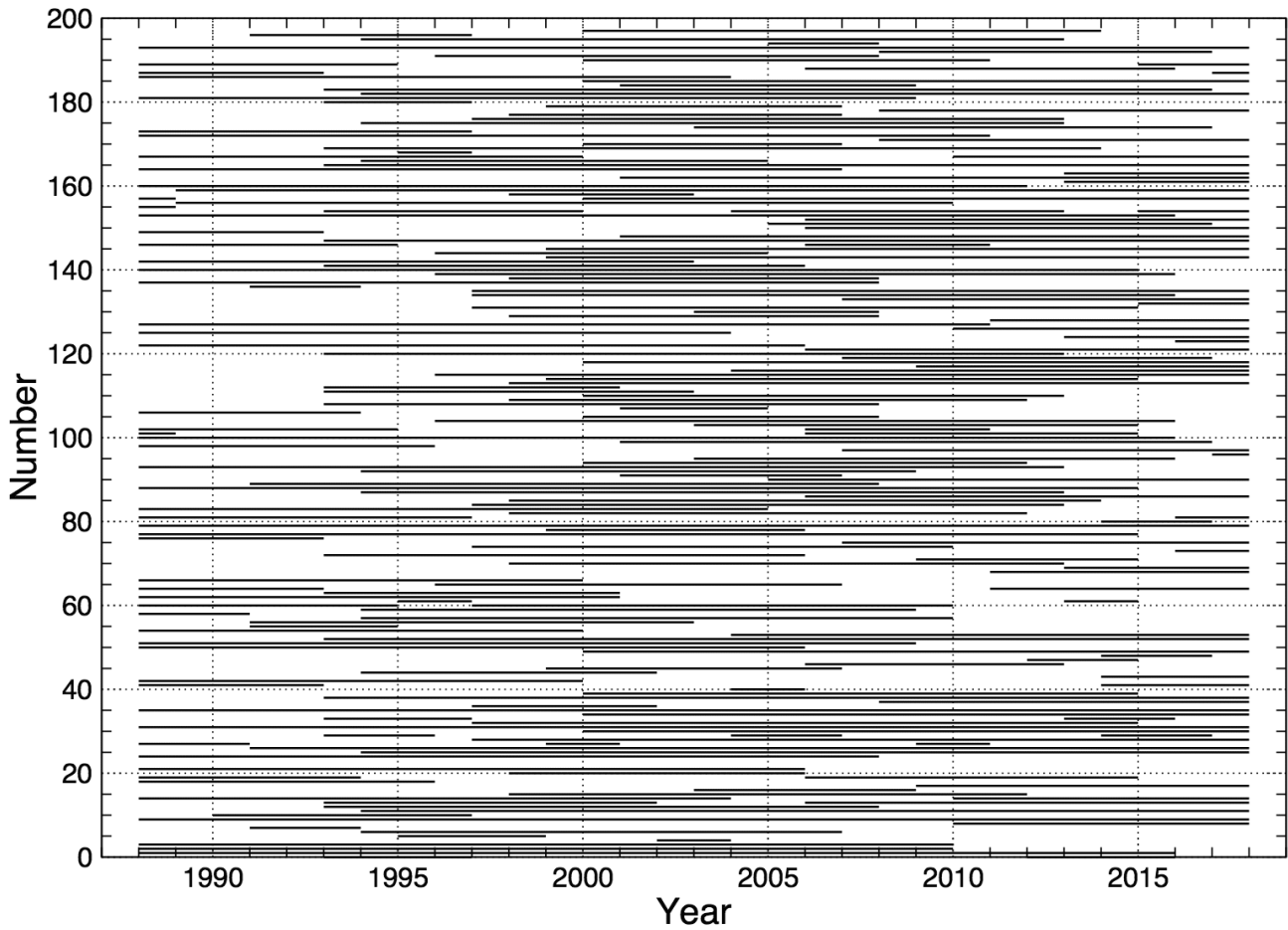
942



943

944 Fig. 11: Comparing topographic characteristics of surging glaciers to all others. a) Scatterplot of the elevation
945 range vs. glacier size. b) Glacier hypsometry for surging and other glaciers.

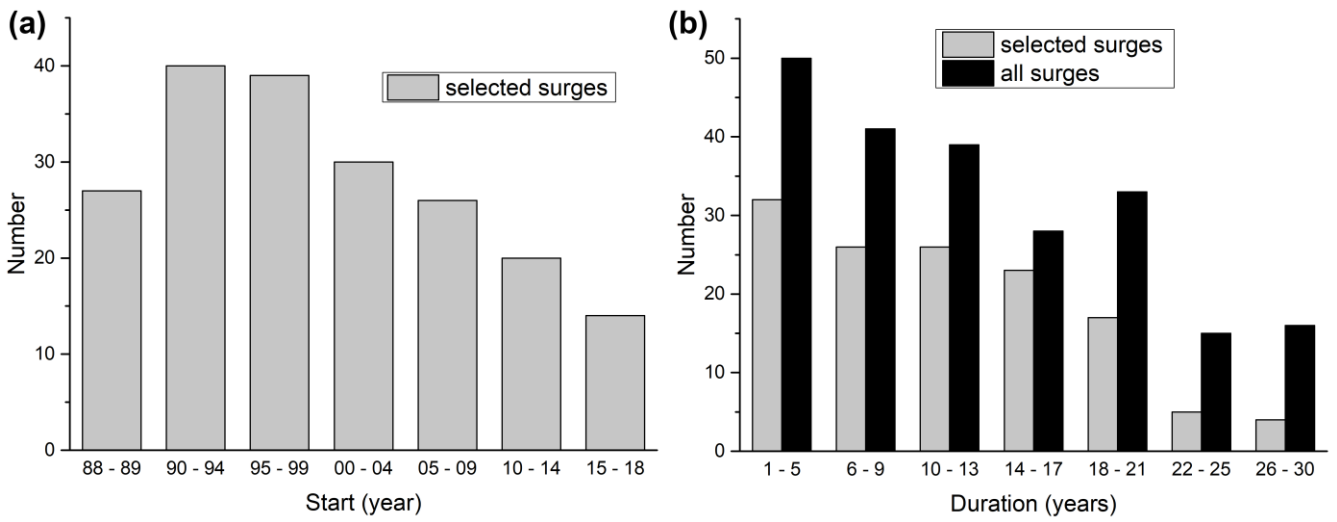
946



947

948 Fig. 12: Surge periods for all glaciers with observed surges (GI-3min). Those starting (ending) in 1988 (2018)
949 might have started earlier / last longer than indicated by the line.

950



951

952 *Fig. 13: Histograms of surge characteristics. a) Periods in which the surges have started, b) surge durations. The*
 953 *charts provide greater detail than the classification code to allow for a better analysis and keep the glacier code*
 954 *in the inventory simple. The “88-89” label in a) includes only glaciers that started surging in 1989 as we cannot*
 955 *be sure about a surge start of 1988 (might also been earlier). The grey bars in b) refer to the surges that*
 956 *occurred completely within the study period, i.e. started after 1988 and ended before 2018.*

957

958